VOTCA-XTP

EXCITON TRANSPORT SIMULATIONS

USER MANUAL

compiled from: 1.4-dev (ad1d776)

September 15, 2016

www.votca.org

Disclamer

This manual is not complete. The best way to start using the software is to look at provided tutorials. The reference section is generated automatically from the source code, so please make sure that your software and manual versions match.

Citations

Development of this software depends on academic research grants. If you are using the package, please cite the following papers

[1] Microscopic simulations of charge transport in disordered organic semiconductors,
Victor Rühle, Alexander Lukyanov, Falk May, Manuel Schrader, Thorsten Vehoff, James Kirkpatrick, Björn Baumeier and Denis Andrienko
J. Chem. Theor. Comp. 7, 3335, 2011

[2] Versatile Object-oriented Toolkit for Coarse-graining Applications
Victor Rühle, Christoph Junghans, Alexander Lukyanov, Kurt Kremer and Denis Andrienko
J. Chem. Theor. Comp. 5, 3211, 2009

Development

The core development is currently taking place at the Max Planck Institute for Polymer Research, Mainz, Germany and TU/e Eindhoven.

Copyright

VOTCA-XTP is free software. The entire package is available under the Apache License. For details, check the LICENSE file in the source code. The VOTCA-XTP source code is available on our homepage, www.votca.org.

Contents

Index

Chapter 1

Introduction

Charge carrier dynamics in an organic semiconductor can often be described in terms of charge hopping between localized states. The hopping rates depend on electronic coupling elements, reorganization energies, and site energies, which vary as a function of position and orientation of the molecules. The purpose of the VOTCA-XTP package [1] is to simplify the workflow for charge transport simulations, provide a uniform error-control for the methods, flexible platform for their development, and eventually allow *in silico* prescreening of organic semiconductors for specific applications.

The toolkit is implemented using modular concepts introduced earlier in the Versatile Object-oriented Toolkit for Coarse-graining Applications (VOTCA) [2]. It contains different programs, which execute specific tasks implemented in calculators representing an individual step in the workflow. Figure 1.1 summarizes a typical chain of commands to perform a charge transport simulation: First, the VOTCA code structures are adapted to reading atomistic trajectories, mapping them onto conjugated segments and rigid fragments, and substituting (if needed) rigid fragments with the optimized copies (`xtp_map`). The programs `xtp_run` and `xtp_parallel` (for heavy-duty tasks) are then used to calculate all bimolecular charge hopping rates (via precalculation of all required ingredients). Site energies (or energetic disorder) can be determined as a combination of internal (ionization potentials/electron affinities of single molecules) as well as electrostatic and polarization contributions within the molecular environment. The calculation of electronic coupling elements between conjugated segments from the corresponding molecular orbitals can be performed using a dimer-projection technique based on density-functional theory (DFT). This requires explicit calculations using quantum-chemistry software for which we provide interfaces to `Gaussian`, `Turbomole`, and `NWChem`. Alternatively, the molecular orbital overlap module calculates electronic coupling elements relying on the semi-empirical INDO Hamiltonian and molecular orbitals in the format provided by the `Gaussian` package.

The kinetic Monte Carlo module reads in the neighbor list, site coordinates, and hopping rates and performs charge dynamics simulations using either periodic boundary conditions or charge sources and sinks.

The toolkit is written as a combination of modular C++ code and scripts. The data transfer between programs is implemented via a state file (sql database), which is also used to restart simulations. Analysis functions and most of the calculation routines are encapsulated by using the observer pattern [3] which allows the implementation of new functions as individual modules.

In the following chapter 2, we summarize the theoretical background of the workflow of charge transport simulations and in particular its individual steps. Chapter 3 describes the structure and content of input and output files, while a full reference of programs and calculators is available in chapter 4. For a hands-on tutorial, the reader is referred to the VOTCA-XTP project page at http://code.google.com/p/votca-xtp/.

3

Figure 1.1: A practical workflow of charge transport simulations using VOTCA-XTP. The theoretical background of the individual steps is given in chapter 2. Chapter 3 describes the content of input and output files, while a full reference of programs and calculators is available in chapter 4.

fig:summary

Chapter 2

Theoretical background

2.1 Workflow

A typical workflow of charge transport simulations is depicted in figure 2.1. The first step is the simulation of an atomistic morphology, which is then partitioned on hopping sites. The coordinates of the hopping sites are used to construct a list of pairs of molecules, or neighbor list.
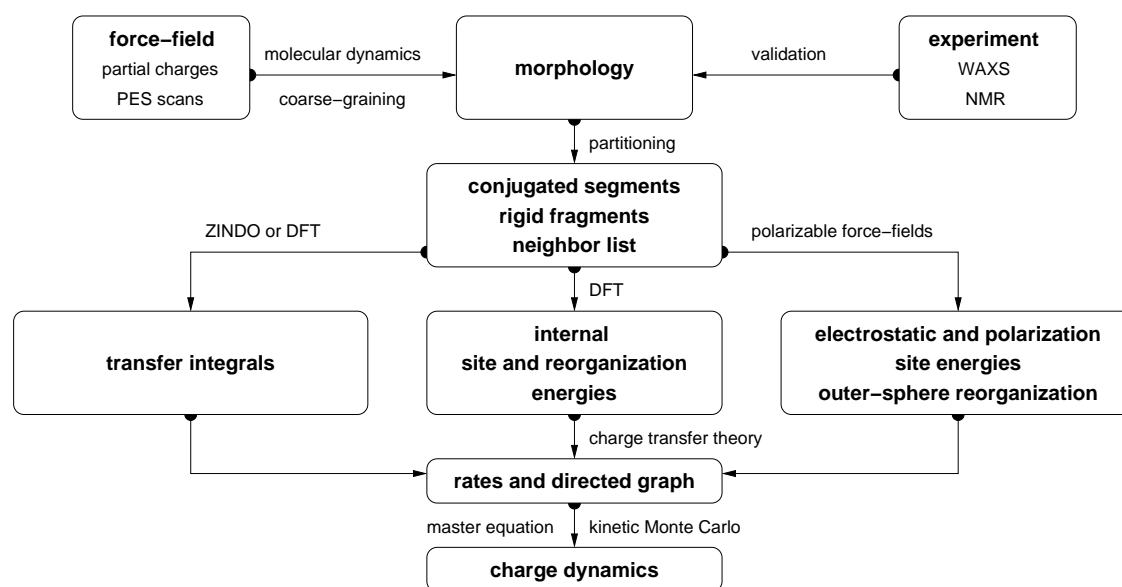
Figure 2.1: Workflow for microscopic simulations of charge transport.

For each pair an electronic coupling element, a reorganization energy, a driving force, and eventually the hopping rate are evaluated. The neighbor list and hopping rates define a directed graph. The corresponding master equation is solved using the kinetic Monte Carlo method, which allows to explicitly monitor the charge dynamics in the system as well as to calculate time or ensemble averages of occupation probabilities, charge fluxes, correlation functions, and field-dependent mobilities.

2.2 Material morphology

There is no generic recipe on how to predict a large-scale atomistically-resolved morphology of an organic semiconductor. The required methods are system-specific: for ultra-pure crystals, for

5

Figure 2.2: The concept of conjugated segments and rigid fragments. Dashed lines indicate conjugated segments while colors denote rigid fragments. (a) Hexabenzocoronene: the π-conjugated system is both a rigid fragment and a conjugated segment. (b) $\mathrm{Alq_3}$: the Al atom and each ligand are rigid fragments while the whole molecule is a conjugated segment. (c) Polythiophene: each repeat unit is a rigid fragment. A conjugated segment consists of one or more rigid fragments. One molecule can have several conjugated segments.

example, density-functional methods can be used provided the crystal structure is known from experiment. For partially disordered organic semiconductors, however, system sizes much larger than a unit cell are required. Classical molecular dynamics or Monte Carlo techniques are then the methods of choice.

In molecular dynamics, atoms are represented by point masses which interact via empirical potentials prescribed by a force-field. Force-fields are parametrized for a limited set of compounds and their refinement is often required for new molecules. In particular, special attention shall be paid to torsion potentials between successive repeat units of conjugated polymers or between functional groups and the π-conjugated system. First-principles methods can be used to characterize the missing terms of the potential energy function.

Self-assembling materials, such as soluble oligomers, discotic liquid crystals, block copolymers, partially crystalline polymers, etc., are the most complicated to study. The morphology of such systems often has several characteristic length scales and can be kinetically arrested in a thermodynamically non-equilibrium state. For such systems, the time- and length-scales of atomistic simulations might be insufficient to equilibrate or sample desired morphologies. In this case, systematic coarse-graining can be used to enhance sampling [2]. Note that the coarse-grained representation must reflect the structure of the atomistic system and allow for back-mapping to the atomistic resolution.

Here we assume that the morphology is already known, that is we know how the topology and the coordinates of all atoms in the systems at a given time. VOTCA-XTP can read standard `GROMACS` topology files. Custom definitions of atomistic topology via XML files are also possible. Since the description of the atomistic topology is the first step in the charge transport simulations, it is important to follow simple conventions on how the system is partitioned on molecules, residues, and how atoms are named in the topology. Required input files are described in section atomistic topology.

2.3 Conjugated segments and rigid fragments

With the morphology at hand, the next step is partitioning the system on hopping sites, or conjugated segments, and calculating charge transfer rates between them. Physically intuitive arguments can be used for the partitioning, which reflects the localization of the wave function of a charge. For most organic semiconductors, the molecular architecture includes relatively rigid, planar π-conjugated systems, which we will refer to as rigid fragments. A conjugated segment can contain one or more of such rigid fragments, which are linked by bonded degrees of freedom.

The dynamics of these degrees of freedom evolves on timescales much slower than the frequency of the internal promoting mode. In some cases, e.g. glasses, it can be 'frozen' due to non-bonded interactions with the surrounding molecules.

To illustrate the concept of conjugated segments and rigid fragments, three representative molecular architectures are shown in figure 2.2. The first one is a typical discotic liquid crystal, hexabenzocoronene. It consists of a conjugated core to which side chains are attached to aid self-assembly and solution processing. In this case the orbitals localized on side chains do not participate in charge transport and the conjugated π-system is both, a rigid fragment and a conjugated segment. In $\mathrm{Alq_3}$, a metal-coordinated compound, a charge carrier is delocalized over all three ligands. Hence, the whole molecule is one conjugated segment. Individual ligands are relatively rigid, while energies of the order of $k_\mathrm{B}T$ are sufficient to reorient them with respect to each other. Thus the Al atom and the three ligands are rigid fragments. In the case of a conjugated polymer, one molecule can consist of several conjugated segments, while each backbone repeat unit is a rigid fragment. Since the conjugation along the backbone can be broken due to large out-of-plane twists between two repeat units, an empirical criterion, based on the dihedral angle, can be used to partition the backbone on conjugated segments [4]. However, such intuitive partitioning is, to some extent, arbitrary and shall be validated by other methods [5–7].

After partitioning, an additional step is often required to remove bond length fluctuations introduced by molecular dynamics simulations, since they are already integrated out in the derivation of the rate expression. This is achieved by substituting respective molecular fragments with rigid, planar π-systems optimized using first-principles methods. Centers of mass and gyration tensors are used to align rigid fragments, though a custom definition of local axes is also possible. Such a procedure also minimizes discrepancies between the force-field and first-principles-based ground state geometries of conjugated segments, which might be important for calculations of electronic couplings, reorganization energies, and intramolecular driving forces.

To partition the system on hopping sites and substitute rigid fragments with the corresponding ground-state geometries `xtp_map` program is used: *`xtp_map -t topol.tpr -c traj.xtc -s map.xml -f state.sql` It reads in the GROMACS topology (`topol.tpr`) and trajectory (`traj.xtc`) files, definitions of conjugated segments and rigid fragments (`map.xml`) and outputs coordinates of conjugated segments (hopping sites) and rigid fragments (as provided in the MD trajectory and after rigidification) to the state file (`state.sql`). In order to do this, a mapping file `map.xml` has to be provided, which specifies the corresponding atoms in the different representations. After this step, all information (frame number, dimensions of the simulation box, etc) are stored in the state file and only this file is used for further calculations.*

VOTCA-XTP requires a wrapped trajectory for mapping the segments and fragments, so all molecules should be whole in the frame.

In order to visually check the mapping one can use either the `tdump` calculator or the programm `xtp_dump` with the calculator `trajectory2pdb`.

`xtp_dump -f state.sql -e trajectory2pdb`

It reads in the state file created by `xtp_map` and outputs two trajectory files corresponding to the original and rigidified atom coordinates. To check the mapping, it is useful to superimpose the three outputs (original atomistic, atomistic stored in the state file, and rigidified according to ground state geometries), e.g., with VMD.

`xtp_run -f state.sql -o options.xml -e tdump`

It also reads in the state file but appends the coordinates to a pdb. file. So make sure to delete old QM.pdb and MD.pdb if you want to create a new imagef

2.4 Neighbor list

A list of neigboring conjugated segments, or neighbor list, contains all pairs of conjugated segments for which coupling elements, reorganization energies, site energy differences, and rates are evaluated.

Two segments are added to this list if the distance between centers of mass of any of their rigid fragments is below a certain cutoff. This allows neighbors to be selected on a criterion of minimum distance of approach
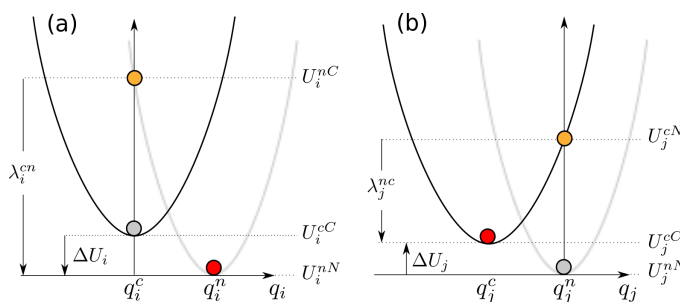
Figure 2.3: Potential energy surfaces of (a) donor and (b) acceptor in charged and neutral states. After the change of the charge state both molecules relax their nuclear coordinates. If all vibrational modes are treated classically, the total internal reorganization energy and the internal energy difference of the electron transfer reaction are $\lambda_{ij}^{\text{int}} = \lambda_i^{cn} + \lambda_j^{nc}$ and $\Delta E_{ij}^{\text{int}} = \Delta U_i - \Delta U_j$, respectively.

rather than center of mass distance, which is useful for molecules with anisotropic shapes.
The neighbor list can be generated from the atomistic trajectory by using the `neighborlist calculator`.
This calculator requires a cutoff, which can be specified in the `options.xml` file. The list is saved to the `state.sql` file: `xtp_run -o options.xml -f state.sql -e neighborlist`

2.5 Reorganization energy

The reorganization energy λ_{ij} takes into account the change in nuclear (and dielectric) degrees of freedom as the charge moves from donor i to acceptor j. It has two contributions: intramolecular, λ_{ij}^{int}, which is due to reorganization of nuclear coordinates of the two molecules forming the charge transfer complex, and intermolecular (outersphere), λ_{ij}^{out}, which is due to the relaxation of the nuclear coordinates of the environment. In what follows we discuss how these contributions can be calculated.

2.5.1 Intramolecular reorganization energy

If intramolecular vibrational modes of the two molecules are treated classically, the rearrangement of their nuclear coordinates after charge transfer results in the dissipation of the internal reorganization energy, λ_{ij}^{int}. It can be computed from four points on the potential energy surfaces (PES) of both molecules in neutral and charged states, as indicated in figure 2.3.
Adding the contributions due to discharging of molecule i and charging of molecule j yields [8]

$$\lambda_{ij}^{int} = \lambda_i^{cn} + \lambda_j^{nc} = U_i^{nC} - U_i^{nN} + U_j^{cN} - U_j^{cC} . \tag{2.1}$$

Here U_i^{nC} is the internal energy of the neutral molecule i in the geometry of its charged state (small n denotes the state and capital C the geometry). Similarly, U_j^{cN} is the energy of the charged molecule j in the geometry of its neutral state. Note that the PES of the donor and acceptor are not identical for chemically different compounds or for conformers of the same molecule. In this case $\lambda_i^{cn} \neq \lambda_j^{cn}$ and $\lambda_i^{nc} \neq \lambda_j^{nc}$. Thus λ_{ij}^{int} is a property of the charge transfer complex, and not of a single molecule.
Intramolecular reorganization energies for discharging (λ^{cn}) and charging (λ^{nc}) of a molecule need to be determined using quantum-chemistry and given in `map.xml`. The values are written to the `state.sql` using the calculator `einternal` (see also `internal energy`): `xtp_run -o options.xml -f state.sql -e einternal`

2.5.2 Outersphere reorganization energy

During the charge transfer reaction, also the molecules outside the charge transfer complex reorient and polarize in order to adjust for changes in electric potential, resulting in the outersphere contribution to the

165 *reorganization energy. λ_{ij}^{out} is particularly important if charge transfer occurs in a polarizable environment.*
166 *Assuming that charge transfer is much slower than electronic polarization but much faster than nuclear*
167 *rearrangement of the environment, λ_{ij}^{out} can be calculated from the electric displacement fields created by*
168 *the charge transfer complex [?]*

$$\lambda_{ij}^{out} = \frac{c_p}{2\epsilon_0} \int_{V^{out}} dV \left[\vec{D}_I(\vec{r}) - \vec{D}_F(\vec{r}) \right]^2 , \tag{2.2}$$

equ:lambda_outer1

169 *where ϵ_0 is the the permittivity of free space, $\vec{D}_{I,F}(\vec{r})$ are the electric displacement fields created by the*
170 *charge transfer complex in the initial (charge on molecule i) and final (charge transferred to molecule j)*
171 *states, V^{out} is the volume outside the complex, and $c_p = \frac{1}{\epsilon_{opt}} - \frac{1}{\epsilon_s}$ is the Pekar factor, which is determined*
172 *by the low (ϵ_s) and high (ϵ_{opt}) frequency dielectric permittivities.*
173 *Eq. (2.2) can be simplified by assuming spherically symmetric charge distributions on molecules i and j*
174 *with total charge e. Integration over the volume V^{out} outside of the two spheres of radii R_i and R_j centered*
175 *on molecules i and j leads to the classical Marcus expression for the outersphere reorganization energy*

$$\lambda_{ij}^{out} = \frac{c_p e^2}{4\pi\epsilon_0} \left(\frac{1}{2R_i} + \frac{1}{2R_j} - \frac{1}{r_{ij}} \right) , \tag{2.3}$$

equ:lambda_outer2

176 *where r_{ij} is the molecular separation. While eq. (2.3) captures the main physics, e.g. predicts smaller*
177 *outer-sphere reorganization energies (higher rates) for molecules at smaller separations, it often cannot*
178 *provide quantitative estimates, since charge distributions are rarely spherically symmetric.*
179 *Alternatively, the displacement fields can be constructed using the atomic partial charges. The difference of*
180 *the displacement fields at the position of an atom b_k outside the charge transfer complex (molecule $k \neq i,j$)*
181 *can be expressed as*

$$\vec{D}_I(\vec{r}_{b_k}) - \vec{D}_F(\vec{r}_{b_k}) = \sum_{a_i} \frac{q_{a_i}^c - q_{a_i}^n}{4\pi} \frac{(\vec{r}_{b_k} - \vec{r}_{a_i})}{|\vec{r}_{b_k} - \vec{r}_{a_i}|^3} + \sum_{a_j} \frac{q_{a_j}^n - q_{a_j}^c}{4\pi} \frac{(\vec{r}_{b_k} - \vec{r}_{a_j})}{|\vec{r}_{b_k} - \vec{r}_{a_j}|^3} , \tag{2.4}$$

182 *where $q_{a_i}^n$ ($q_{a_i}^c$) is the partial charge of atom a of the neutral (charged) molecule i in vacuum. The partial*
183 *charges of neutral and charged molecules are obtained by fitting their values to reproduce the electrostatic*
184 *potential of a single molecule (charged or neutral) in vacuum. Assuming a uniform density of atoms, the*
185 *integration in eq. (2.2) can be rewritten as a density-weighted sum over all atoms excluding those of the*
186 *charge transfer complex.*
187 *The remaining unknown needed to calculate λ_{ij}^{out} is the Pekar factor, c_p. In polar solvents $\epsilon_s \gg \epsilon_{opt} \sim 1$*
188 *and c_p is of the order of 1. In most organic semiconductors, however, molecular orientations are fixed and*
189 *therefore the low frequency dielectric permittivity is of the same order of magnitude as ϵ_{opt}. Hence, c_p is*
190 *small and its value is very sensitive to differences in the permittivities.*
191 *Outersphere reorganization energies for all pairs of molecules in the neighbor list can be computed from*
192 *the atomistic trajectory by using the `eoutersphere` calculator.*
193 *Two methods can be used to compute λ_{ij}^{out}. The first method uses the atomistic partial charges of neutral*
194 *and charged molecules from files specified in `map.xml` and eq. (2.2). The Pekar factor c_p and a cutoff*
195 *radius based on molecular centers of mass have to be specified in the `options.xml` file.*
196 *If this method is computationally prohibitive, λ_{ij}^{out} can be computed using eq. (2.3), which assumes spherical*
197 *charge distributions on the molecules. In this case the radii of these spheres are specified in `segments.xml`,*
198 *while the Pekar factor c_p is given in the `options.xml` file and no cutoff radius is needed.*
199 *The outer sphere reorganization energies are saved to the `state.sql` file: `xtp_run -o options.xml`*
200 *`-f state.sql -e outersphere`*

201 2.6 Site energies

202 *A charge transfer reaction between molecules i and j is driven by the site energy difference, $\Delta E_{ij} =$*
203 *$E_i - E_j$. Since the transfer rate, ω_{ij}, depends exponentially on ΔE_{ij} (see eq. (2.31)) it is important*
204 *to compute its distribution as accurately as possible. The total site energy difference has contributions*

due to *externally applied electric field*, *electrostatic interactions*, polarization effects, and *internal energy* differences. In what follows we discuss how to estimate these contributions by making use of first-principles calculations and polarizable force-fields.

2.6.1   Externally applied electric field

sec:ext_field

The contribution to the total site energy difference due to an external electric field $\vec{F}$ is given by $\Delta E_{ij}^{ext} = q\vec{F} \cdot \vec{r}_{ij}$, where $q = \pm e$ is the charge and $\vec{r}_{ij} = \vec{r}_i - \vec{r}_j$ is a vector connecting molecules i and j. For typical distances between small molecules, which are of the order of $1\,\text{nm}$, and moderate fields of $F < 10^8\,\text{V/m}$ this term is always smaller than $0.1\,\text{eV}$.

2.6.2   Internal energy

sec:internal_energy

The contribution to the site energy difference due to different internal energies (see figure 2.3) can be written as

$$\Delta E_{ij}^{int} = \Delta U_i - \Delta U_j = \left(U_i^{cC} - U_i^{nN} \right) - \left(U_j^{cC} - U_j^{nN} \right) , \tag{2.5}$$

equ:conformational

where $U_i^{cC(nN)}$ is the total energy of molecule i in the charged (neutral) state and geometry. ΔU_i corresponds to the adiabatic ionization potential (or electron affinity) of molecule i, as shown in figure 2.3. For one-component systems and negligible conformational changes $\Delta E_{ij}^{int} = 0$, while it is significant for donor-acceptor systems.

Internal energies determined using quantum-chemistry need to be specified in `map.xml`. The values are written to the `state.sql` using the calculator `einternal` (see also *intramolecular reorganization energy*): `xtp_run -o options.xml -f state.sql -e einternal`

2.6.3   Electrostatic interaction energy

sec:distributed_multipoles

We represent the molecular charge density by choosing multiple expansion sites ("polar sites") per molecule in such a way as to accurately reproduce the molecular electrostatic potential (ESP), with a set of suitably chosen multipole moments $\{Q_{lk}^a\}$ (in spherical-tensor notation) allocated to each site. The expression for the electrostatic interaction energy between two molecules A and B in the multi-point expansion includes an implicit sum over expansion sites $a\epsilon A$ and $b\epsilon B$,

$$U_{AB} = \sum_{a \epsilon A} \sum_{b \epsilon B} \hat{Q}_{l_1 k_1}^a T_{l_1 k_1 l_2 k_2}^{a,b} \hat{Q}_{l_2 k_2}^b \equiv \hat{Q}_{l_1 k_1}^a T_{l_1 k_1 l_2 k_2}^{a,b} \hat{Q}_{l_2 k_2}^b, \tag{2.6}$$

equ:mol_distributed_U

where we have used the Einstein sum convention for the site indices a and b on the right-hand side of the equation, in addition to the sum convention that is in place for the multipole-moment components $t \equiv l_1 k_1$ and $u \equiv l_2 k_2$. The $T_{l_1 k_1 l_2 k_2}^{a,b}$ are tensors that mediate the interaction between a multipole component $l_1 k_1$ on site a with the moment $l_2 k_2$ on site b. If we include the molecular environment into a perturbative term W to enter in the single-molecule Hamiltonian, the above expression is exactly the first-order correction to the energy where the quantum-mechanical detail has been absorbed in classical multipole moments.

The are a number of strategies how to arrive at such a collection of distributed multipoles. They can be classified according to whether the multipoles are derived (a) from the electrostatic potential generated by the SCF charge density or (b) from a decomposition of the wavefunction itself. Here, we will only draft two of those approaches, CHELPG [9] from category (a) and DMA [10] from category (b).

The CHELPG (CHarges from ELectrostatic Potentials, Grid-based) method relies on performing a least-squares fit of atom-placed charges to reproduce the electrostatic potential as evaluated from the SCF density on a regularly spaced grid [9]. The fitted charges result from minimizing the Lagrangian function [11]

$$z(\{q_i\}) = \sum_{k=1}^{M} \left(\phi(\vec{r}_k) - \sum_{i=1}^{N} \frac{1}{4\pi\varepsilon_0} \frac{q_i}{|\vec{r}_i - \vec{r}_k|} \right) + \lambda \left(q_{mol} - \sum_{i=1}^{N} q_i \right) , \tag{2.7}$$

234 *with M grid points, N atomic sites, the set of atomic partial charges $\{q_i\}$ and the SCF potential ϕ. The*
235 *Lagrange multiplier λ constrains the sum of the fitted charges to the molecular charge q_{mol}. The main*
236 *difference from other fitting schemes [12] is the algorithm that selects the positions at which the potential is*
237 *evaluated (we note that the choice of grid points can have substantial effects especially for bulky molecules).*
238 *Clearly, the CHELPG method can be (and has been) extended to include higher atomic multipoles. It should*
239 *be noted, however, how already the inclusion of atomic dipoles hardly improves the parametrization, and*
240 *can in fact be harmful to its conformational stability.*

The Distributed-Multipole-Analysis (DMA) approach [10, 13], developed by A. Stone, operates directly
on the quantum-mechanical density matrix, expanded in terms of atom- and bond-centered Gaussian func-
tions $\chi_\alpha = R_{LK}(\vec{x} - \vec{s}_\alpha) \exp[-\zeta(\vec{x} - \vec{s}_\alpha)^2]$,

$$\rho(\vec{x}) = \sum_{\alpha,\beta} \rho_{\alpha\beta} \chi_\alpha(\vec{x} - \vec{s}_\alpha) \chi_\beta(\vec{x} - \vec{s}_\beta). \tag{2.8}$$

The aim is to compute multipole moments according in a distributed fashion: If we use that the over-
lap product $\chi_\alpha \chi_\beta$ of two Gaussian basis functions yields itself a Gaussian centered at $\vec{P} = (\zeta_\alpha \vec{s}_\alpha + \zeta_\beta \vec{s}_\beta)/(\zeta_\alpha + \zeta_\beta)$, it is possible to proceed in two steps: First, we compute the multipole moments associ-
ated with a specific summand in the density matrix, referred to the overlap center $\vec{P}$:

$$Q_{LK}[\vec{P}] = -\int R_{LK}(\vec{x} - \vec{P}) \rho_{\alpha\beta} \chi_\alpha \chi_\beta d^3x. \tag{2.9}$$

Second, we transfer the resulting $Q_{lk}[\vec{P}]$ to the position $\vec{S}$ of a polar site according to the rule [10]

$$Q_{nm}[\vec{S}] = \sum_{l=0}^{L} \sum_{k=-l}^{l} \left[\begin{pmatrix} n+m \\ l+k \end{pmatrix} \begin{pmatrix} n-m \\ l-k \end{pmatrix} \right]^{1/2} R_{n-l,m-k}(\vec{S} - \vec{P}) \cdot Q_{lk}[\vec{P}]. \tag{2.10}$$

241 *Note how this requires a rule for the choice of the expansion site to which the multipole moment should*
242 *be transferred. In the near past [13], the nearest-site algorithm, which allocates the multipole moments to*
243 *the site closest to the overlap center, was replaced for diffuse functions by an algorithm based on a sxtpth*
244 *weighting function in conjunction with grid-based integration methods in order to decrease the basis-set*
245 *dependence of the resulting set of distributed multipoles.*
246 *One important advantage of the DMA approach over fitting algorithms such as CHELPG or Merz-*
247 *Kollman (MK) is that higher-order moments can also be derived without too large an ambiguity.*
248 *The 'mps' file format used by VOTCA for the definition of distributed multipoles (as well as point polariz-*
249 *abilities, see subsequent section) is based on the GDMA punch format of A. Stone's GDMA program [13]*
250 *(the punch output file can be immediately plugged into VOTCA without any conversions to be applied).*
251 *Furthermore the log-file of different QM packages (currently* `Gaussian`*,* `Turbomole` *and* `NWChem`*)*
252 *may be fed into the* `log2mps` *tool, which will subsequently generate the appropriate mps-file.*
253 `xtp_tools -o options.xml -e log2mps`

2.6.4 Induction energy - the Thole model
254

If we in addition to the permanent set of multipole moments $\{Q_t^a\}$ allow for induced moments $\{\Delta Q_t^a\}$ and
penalize their generation with a bilinear form (giving rise to a strictly positive contribution to the energy),

$$U_{int} = \frac{1}{2} \sum_A \Delta Q_t^a \eta_{tt'}^{aa'} \Delta Q_{t'}^{a'}, \tag{2.11}$$

it can be shown that the induction contribution to the site energy evaluates to an expression where all in-
teractions between induced moments have cancelled out, and interactions between permanent and induced
moments are scaled down by $1/2$ [14]:

$$U_{pu} = \frac{1}{2} \sum_A \sum_{B>A} \left[\Delta Q_t^a T_{tu}^{ab} Q_u^b + \Delta Q_t^b T_{tu}^{ab} Q_u^a \right]. \tag{2.12}$$

This term can be viewed as the second-order (induction) correction to the molecular interaction energy.
The sets of $\{Q_t^a\}$ are solved for self-consistently via

$$\Delta Q_t^a = - \sum_{B \neq A} \alpha_{tt'}^{aa'} T_{t'u}^{a'b} (Q_u^b + \Delta Q_u^b),$$ (2.13) equ:self_consistent_dQ

255 *where the polarizability tensors $\alpha_{tt'}^{aa'}$ are given by the inverse of $\eta_{tt'}^{aa'}$.*
256 *With eqs. 2.13 and 2.12 we have at hand expressions that allow us to compute the induction energy contri-*
257 *bution to site energies in an iterative manner based on a set of molecular distributed multipoles $\{Q_t^a\}$ and*
258 *polarizabilities $\{\alpha_{tt'}^{aa'}\}$. We have drafted in the previous section how to obtain the former from a wavefunc-*
259 *tion decomposition or fitting scheme (GDMA, CHELPG). The $\{\alpha_{tt'}^{aa'}\}$ can be derived formally (or rather:*
260 *read off) from a perturbative expansion of the molecular interaction. In this work we make use of the Thole*
261 *model [15?] as a semi-empirical approach to obtain the sought-after point polarizabilities in the local*
262 *dipole approximation, that is, $[\alpha_{tt'}^{aa'}] = \alpha_{tt'}^{aa'} \delta_{t\beta} \delta_{t'\beta} \delta_{aa'}$, where $\beta \epsilon \{x, y, z\}$ references the dipole-moment*
263 *component.*
264 *The Thole model is based on a modified dipole-dipole interaction, which can be reformulated in terms of the*
265 *interaction of smeared charge densities. This has been shown to be necessary due to the divergent head-*
266 *to-tail dipole-dipole interaction that otherwise results at small interseparations on the Å scale [15? ?].*
267 *Smearing out the charge distribution mimics the nature of the QM wavefunction, which effectively guards*
268 *against this unphysical polarization catastrophe. Since the point dipoles however only react individually*
269 *to the external field, any correlation effects as were still accounted for in the $\{\alpha_{tt'}^{aa'}\}$ are lost, except perhaps*
270 *those correlations that are due to the mere classical field interaction.*
The smearing of the nuclei-centered multipole moments is obtained via a fractional charge density $\rho_f(\vec{u})$
which should be normalized to unity and fall off rapidly as of a certain radius $\vec{u} = \vec{u}(\vec{R})$. The latter is
related to the physical distance vector $\vec{R}$ connecting two interacting sites via a linear scaling factor that
takes into account the magnitude of the isotropic site polarizabilities α^a. This isotropic fractional charge
density gives rise to a modified potential

$$\phi(u) = -\frac{1}{4\pi\varepsilon_0} \int_0^u 4\pi u' \rho(u') du'$$ (2.14) equ:mod_potential

We can relate the multipole interaction tensor $T_{ij...}$ (this time in Cartesian coordinates) to the fractional
charge density in two steps: First, we rewrite the tensor in terms of the scaled distance vector $\vec{u}$,

$$T_{ij...}(\vec{R}) = f(\alpha^a \alpha^b) \, t_{ij...}(\vec{u}(\vec{R}, \alpha^a \alpha^b)),$$ (2.15)

where the specific form of $f(\alpha^a \alpha^b)$ results from the choice of $u(\vec{R}, \alpha^a \alpha^b)$. Second, we demand that the
smeared interaction tensor $t_{ij...}$ is given as usual by the appropriate derivative of the potential in eq. 2.14,

$$t_{ij...}(\vec{u}) = -\partial_{u_i} \partial_{u_j} \ldots \phi(\vec{u}).$$ (2.16)

271 *It turns out that for a suitable choice of $\rho_f(\vec{u})$, the modified interaction tensors can be rewritten in such a*
272 *way that powers n of the distance $R = |\vec{R}|$ are damped with a damping function $\lambda_n(\vec{u}(\vec{R}))$ [16].*
273 *There is a large number of fractional charge densities $\rho_f(\vec{u})$ that have been tested for the purpose of giving*
274 *best results for the molecular polarizability as well as interaction energies. Note how a great advantage*
275 *of the Thole model is the exceptional transferability of the atomic polarizabilities to compounds not used*
276 *for the fitting procedure [?]. In fact, for most organic molecules, a fixed set of atomic polarizabilities*
277 *($\alpha_C = 1.334$, $\alpha_H = 0.496$, $\alpha_N = 1.073$, $\alpha_O = 0.873$, $\alpha_S = 2.926$ Å^3) based on atomic elements yields*
278 *satisfactory results.*
VOTCA implements the Thole model with an exponentially-decaying fractional charge density

$$\rho(u) = \frac{3a}{4\pi} \exp(-au^3),$$ (2.17)

279 *where $\vec{u}(\vec{R}, \alpha^a \alpha^b) = \vec{R}/(\alpha^a \alpha^b)^{1/6}$ and the smearing exponent $a = 0.39$ (which can however be changed*
280 *from the program options), as used in the AMOEBA force field [16].*
281 *Even though the Thole model performs very well for many organic compounds with only the above small set*
282 *of element-based polarizabilities, conjugated molecules may require a more intricate parametrization. The*
283 *simplest approach is to resort to scaled polarizabilities to match the effective molecular polarizable volume*
284 *$V \sim \alpha_x \alpha_y \alpha_z$ as predicted by QM calculations (here $\alpha_x, \alpha_y, \alpha_z$ are the eigenvalues of the molecular*
285 *polarizability tensor). The* `molpol tool` *assists with this task, it self-consistently calculates the Thole*
286 *polarizability for an input mps-file and optimizes (if desired) the atomic polarizabilities in the above simple*
287 *manner.*
288 `xtp_tools -o options.xml -e molpol`
289 *The electrostatic and induction contribution to the site energy is evaluated by the* `emultipole calculator`.
290 *Atomistic partial charges for charged and neutral molecules are taken from mps-files (extended GDMA*
291 *format) specified in* `map.xml`. *Note that, in order to speed up calculations for both methods, a cut-off*
292 *radius (for the molecular centers of mass) can be given in* `options.xml`. *Threaded execution is advised.*
293 `xtp_run -o options.xml -f state.sql -e emultipole`
294 *Furthermore available are* `zmultipole`, *which extends* `emultipole` *to allow for an electrostatic buffer*
295 *layer (loosely related to the z-buffer in OpenGL, hence the name) and anisotropic point polarizabilities. For*
296 *the interaction energy of charged clusters of any user-defined composition (Frenkel states, CT states, ...),*
297 `xqmultipole` *can be used.*
298 `xtp_parallel -o options.xml -f state.sql -e xqmultipole`

299 2.7 Transfer integrals

300 *The electronic transfer integral element J_{ij} entering the Marcus rates in eq. (2.31) is defined as*

$$J_{ij} = \left\langle \phi_i \left| \hat{H} \right| \phi_j \right\rangle, \tag{2.18}$$

301 *where ϕ_i and ϕ_j are diabatic wavefunctions, localized on molecule i and j respectively, participating in the*
302 *charge transfer, and $\hat{H}$ is the Hamiltonian of the formed dimer. Within the frozen-core approximation, the*
303 *usual choice for the diabatic wavefunctions ϕ_i is the highest occupied molecular orbital (HOMO) in case of*
304 *hole transport, and the lowest unoccupied molecular orbital (LUMO) in the case of electron transfer, while*
305 *$\hat{H}$ is an effective single particle Hamiltonian, e.g. Fock or Kohn-Sham operator of the dimer. As such, J_{ij}*
306 *is a measure of the strength of the electronic coupling of the frontier orbitals of monomers mediated by the*
307 *dimer interactions.*
308 *Intrinsically, the transfer integral is very sensitive to the molecular arrangement, i.e. the distance and the*
309 *mutual orientation of the molecules participating in charge transport. Since this arrangement can also*
310 *be significantly influenced by static and/or dynamic disorder [17**? ? **–19], it is essential to calculate J_{ij}*
311 *explicitly for each hopping pair within a realistic morphology. Considering that the number of dimers for*
312 *which eq. (2.18) has to be evaluated is proportional to the number of molecules times their coordination*
313 *number, computationally efficient and at the same time quantitatively reliable schemes are required.*

314 2.7.1 Projection of monomer orbitals on dimer orbitals (DIPRO)

315 *An approach for the determination of the transfer integral that can be used for any single-particle electronic*
316 *structure method (Hartree-Fock, DFT, or semiempirical methods) is based on the projection of monomer*
317 *orbitals on a manifold of explicitly calculated dimer orbitals. This dimer projection (DIPRO) technique in-*
318 *cluding an assessment of computational parameters such as the basis set, exchange-correlation functionals,*
319 *and convergence criteria is presented in detail in ref. [20]. A brief summary of the concept is given below.*
320 *We start from an effective Hamiltonian* [1]

$$\hat{H}^{eff} = \sum_i \epsilon_i \hat{a}_i^\dagger \hat{a}_i + \sum_{j \neq i} J_{ij} \hat{a}_i^\dagger \hat{a}_j + c.c. \tag{2.19}$$

---

[1] we use following notations: a - number, $\bar{a}$ - vector, $\mathbf{A}$ - matrix, $\hat{A}$ - operator

where $\hat{a}_i^\dagger$ and $\hat{a}_i$ are the creation and annihilation operators for a charge carrier located at the molecular site i. The electron site energy is given by ϵ_i, while J_{ij} is the transfer integral between two sites i and j. We label their frontier orbitals (HOMO for hole transfer, LUMO for electron transfer) ϕ_i and ϕ_j, respectively. Assuming that the frontier orbitals of a dimer (adiabatic energy surfaces) result exclusively from the interaction of the frontier orbitals of monomers, and consequently expand them in terms of ϕ_i and ϕ_j. The expansion coefficients, $\bar{\mathbf{C}}$, can be determined by solving the secular equation

$$(\mathbf{H} - E\mathbf{S})\bar{\mathbf{C}} = 0 \tag{2.20}$$

where $\mathbf{H}$ and $\mathbf{S}$ are the Hamiltonian and overlap matrices of the system, respectively. These matrices can be written explicitly as

$$\mathbf{H} = \begin{pmatrix} e_i & H_{ij} \\ H_{ij}^* & e_j \end{pmatrix} \qquad\qquad \mathbf{S} = \begin{pmatrix} 1 & S_{ij} \\ S_{ij}^* & 1 \end{pmatrix} \tag{2.21}$$

with

$$\begin{aligned} e_i &= \langle \phi_i | \hat{H} | \phi_i \rangle & H_{ij} &= \langle \phi_i | \hat{H} | \phi_j \rangle \\ e_j &= \langle \phi_j | \hat{H} | \phi_j \rangle & S_{ij} &= \langle \phi_j | \phi_j \rangle \end{aligned} \tag{2.22}$$

The matrix elements $e_{i(j)}$, H_{ij}, and S_{ij} entering eq. (2.21) can be calculated via projections on the dimer orbitals (eigenfunctions of $\hat{H}$) $\{|\phi_n^D\rangle\}$ by inserting $\hat{1} = \sum_n |\phi_n^D\rangle \langle \phi_n^D|$ twice. We exemplify this explicitly for H_{ij} in the following

$$H_{ij} = \sum_{nm} \langle \phi_i | \phi_n^D \rangle \langle \phi_n^D | \hat{H} | \phi_m^D \rangle \langle \phi_m^D | \phi_j \rangle. \tag{2.23}$$

The Hamiltonian is diagonal in its eigenfunctions, $\langle \phi_n^D | \hat{H} | \phi_m^D \rangle = E_n \delta_{nm}$. Collecting the projections of the frontier orbitals $|\phi_{i(j)}\rangle$ on the n-th dimer state $(\bar{\mathbf{V}}_{(i)})_n = \langle \phi_i | \phi_n^D \rangle$ and $(\bar{\mathbf{V}}_{(j)})_n = \langle \phi_j | \phi_n^D \rangle$ respectively, into vectors we obtain

$$H_{ij} = \bar{\mathbf{V}}_{(i)} \mathbf{E} \bar{\mathbf{V}}_{(j)}^\dagger. \tag{2.24}$$

What is left to do is determine these projections $\bar{\mathbf{V}}_{(k)}$. In all practical calculations the molecular orbitals are expanded in basis sets of either plane waves or of localized atomic orbitals $|\varphi_\alpha\rangle$. We will first consider the case that the calculations for the monomers are performed using a counterpoise basis set that is commonly used to deal with the basis set superposition error (BSSE). The basis set of atom-centered orbitals of a monomer is extended to the one of the dimer by adding the respective atomic orbitals at virtual coordinates of the second monomer. We can then write the respective expansions as

$$|\phi_k\rangle = \sum_\alpha \lambda_\alpha^{(k)} |\varphi_\alpha\rangle \qquad and \qquad |\phi_n^D\rangle = \sum_\alpha D_\alpha^{(n)} |\varphi_\alpha\rangle \tag{2.25}$$

where $k = i, j$. The projections can then be determined within this common basis set as

$$\left(\bar{\mathbf{V}}_k\right)_n = \langle \phi_k | \phi_n^D \rangle = \sum_\alpha \lambda_\alpha^{(k)} \langle \alpha | \sum_\beta D_\beta^{(n)} |\beta\rangle = \bar{\boldsymbol{\lambda}}_{(k)}^\dagger \mathcal{S} \bar{\mathbf{D}}_{(n)} \tag{2.26}$$

where $\mathcal{S}$ is the overlap matrix of the atomic basis functions. This allows us to finally write the elements of the Hamiltonian and overlap matrices in eq. (2.21) as:

$$\begin{aligned} H_{ij} &= \bar{\boldsymbol{\lambda}}_{(i)}^\dagger \mathcal{S} \mathbf{D} \mathbf{E} \mathbf{D}^\dagger \mathcal{S}^\dagger \bar{\boldsymbol{\lambda}}_{(j)} \\ S_{ij} &= \bar{\boldsymbol{\lambda}}_{(i)}^\dagger \mathcal{S} \mathbf{D} \mathbf{D}^\dagger \mathcal{S}^\dagger \bar{\boldsymbol{\lambda}}_{(j)} \end{aligned} \tag{2.27}$$

Since the two monomer frontier orbitals that form the basis of this expansion are not orthogonal in general ($\mathbf{S} \neq \mathbf{1}$), it is necessary to transform eq. (2.20) into a standard eigenvalue problem of the form

$$\mathbf{H}^{\text{eff}} \bar{\mathbf{C}}^{\text{eff}} = E \bar{\mathbf{C}}^{\text{eff}} \tag{2.28}$$

347 *to make it correspond to eq.* (2.19). *According to Löwdin such a transformation can be achieved by*

$$\mathbf{H}^{\text{eff}} = \mathbf{S}^{-1/2} \mathbf{H} \mathbf{S}^{-1/2}.$$

(2.29) eq:dipro_eq9

348 *This then yields an effective Hamiltonian matrix in an orthogonal basis, and its entries can directly be*
349 *identified with the site energies ϵ_i and transfer integrals J_{ij}:*

$$\mathbf{H}^{\text{eff}} = \begin{pmatrix} e_i^{\text{eff}} & H_{ij}^{\text{eff}} \\ H_{ij}^{*,\text{eff}} & e_j^{\text{eff}} \end{pmatrix} = \begin{pmatrix} \epsilon_i & J_{ij} \\ J_{ij}^* & \epsilon_j \end{pmatrix}$$

(2.30) eq:dipro_eq11
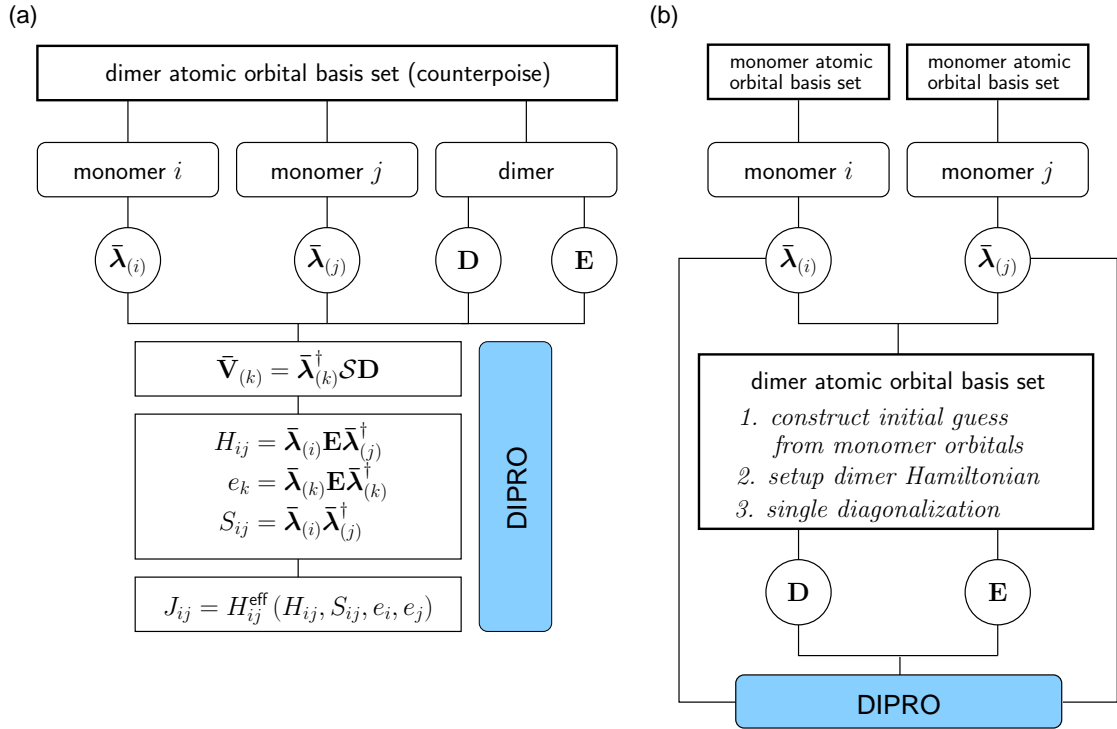
Figure 2.4: Schematics of the DIPRO method. (a) General workflow of the projection technique. (b) Strategy of the efficient noCP+noSCF implementation, in which the monomer calculations are performed independently form the dimer configurations (noCP), using the `edft` calculator. The dimer Hamiltonian is subsequently constructed based on an initial guess formed from monomer orbitals and only diagonalized once (noSCF) before the transfer integral is calculated by projection. This second step is performed by the `idft` calculator.

fig:dipro_scheme

2.7.2 DFT-based transfer integrals using DIPRO

350

sec:dft

351 *The calculation of one electronic coupling element based on DFT using the `DIPRO` method requires the*
352 *overlap matrix of atomic orbitals $\mathcal{S}$, the expansion coefficients for monomer $\bar{\boldsymbol{\lambda}}_{(k)} = \{\lambda_\alpha^{(k)}\}$ and dimer*
353 *orbitals $\bar{\mathbf{D}}_{(n)} = \{D_\alpha^{(n)}\}$, as well as the orbital energies E_n of the dimer are required as input. In practical*
354 *situations, performing self-consistent quantum-chemical calculations for each individual monomer and*
355 *one for the dimer to obtain this input data is extremely demanding. Several simplifications can be made*
356 *to reduce the computational effort, such as using non-Counterpoise basis sets for the monomers (thereby*
357 *decoupling the monomer calculations from the dimer run) and performing only a single SCF step in a*
358 *dimer calculation starting from an initial guess formed from a superposition of monomer orbitals. This*

"noCP+noSCF" variant of DIPRO *is shown in figure 2.4(a) and recommended for production runs. A detailed comparative study of the different variants can be found in [20].*

The code currently contains supports evaluation of transfer integrals from quantum-chemical calculations performed with the Gaussian, Turbomole, *and* NWChem *packages. The interfacing procedure consists of three main steps: generation of input files for monomers and dimers, performing the actual quantum-chemical calculations, and calculating the transfer integrals.*

Monomer calculations

First, hopping sites *and a* neighbor list *need to be generated from the atomistic topology and trajectory and written to the* state.sql *file. Then the parallel* edft calculator *manages the calculation of the monomer properties required for the determination of electronic coupling elements. Specifically, the individual steps it performs are:*

1. *Creation of a job file containing the list of molecules to be calculated with DFT* xtp_parallel -o options.xml -f state.sql -e edft -j write

2. *Running of all jobs in job file* xtp_parallel -o options.xml -f state.sql -e edft -j run *which includes*

   - *creating the input files for the DFT calculation (using the package specified in* options.xml*) in the directory*

     OR_FILES/package/frame_F/mol_M

     where F *is the index of the frame in the trajectory,* M *is the index of a molecule in this frame,*

   - *executing the DFT run, and*

   - *after completion of this run, parsing the output (number of electrons, basis set, molecular orbital expansion coefficients), and saving it in compressed form to*

     OR_FILES/molecules/frame_F/molecule_M.orb

Calculating the transfer integrals

After the momomer calculations have been completed successfully, the respective runs for dimers from the neighborlist can be performed using the parallel idft calculator, *which manages the DFT runs for the hopping pairs and determines the coupling element using* DIPRO. *Again, several steps are required:*

1. *Creation of a job file containing the list of pairs to be calculated with DFT* xtp_parallel -o options.xml -f state.sql -e idft -j write

2. *Running of all jobs in job file* xtp_parallel -o options.xml -f state.sql -e idft -j run *which includes*

   - *creating the input files (including the merged guess for a noSCF calculation, if requested) for the DFT calculation (using the package specified in* options.xml*) in the directory*

     OR_FILES/package/frame_F/pair_M_N

     where M *and* N *are the indices of the molecules in this pair,*

   - *executing the DFT run, and*

   - *after completion of this run, parsing the output (number of electrons, basis set, molecular orbital expansion coefficients and energies, atomic orbital overlap matrix), and saving the pair information in compressed form to*

     OR_FILES/pairs/frame_F/pair_M_N.orb

   - *loading the monomer orbitals from the previously saved* *.orb files.

- *calculating the coupling elements and write them to the job file*

3. *Reading the coupling elements from the job file and saving them to the* `state.sql` *file* `xtp_parallel` `-o options.xml -f state.sql -e idft -j read`

2.7.3 ZINDO-based transfer integrals using MOO

An approximate method based on Zerner's Intermediate Neglect of Differential Overlap (ZINDO) has been described in Ref. [21]. This semiempirical method is substantially faster than first-principles approaches, since it avoids the self-consistent calculations on each individual monomer and dimer. This allows to construct the matrix elements of the ZINDO Hamiltonian of the dimer from the weighted overlap of molecular orbitals of the two monomers. Together with the introduction of rigid segments, only a single self-consistent calculation on one isolated conjugated segment is required. All relevant molecular overlaps can then be constructed from the obtained molecular orbitals.

The main advantage of the molecular orbital overlap (MOO) library is fast *evaluation of electronic coupling elements. Note that MOO is based on the ZINDO Hamiltonian which has limited applicability. The general advice is to first compare the accuracy of the MOO method to the DFT-based calculations.*

MOO can be used both in a standalone mode *and as an* `izindo calculator` *of VOTCA-XTP.*

Since MOO constructs the Fock operator of a dimer from the molecular orbitals of monomers by translating and rotating the orbitals of rigid fragments*, the optimized geometry of all* conjugated segments *and the coefficients of the molecular orbitals are required as its input in addition to the state file (*`state.sql`*) with the* neighbor list*. Coordinates are stored in* `geometry.xyz` *files with four columns, first being the atom type and the next three atom coordinates. This is a standard* `xyz` *format without a header. Note that the atom order in the* `geometry.xyz` *files can be different from that of the mapping files. The correspondence between the two is established in the* `map.xml` *file.*

Izindo requires the specification of orbitals for hole and electron transport in `map.xml`*. They are the HOMO and LUMO respectively and can be retrieved from the* `log` *file from which the* `zindo.orb` *file is generated. The number of* `alpha electrons` *is the HOMO, the LUMO is HOMO+1*

The calculated transfer integrals are immediately saved to the `state.sql` *file.* `xtp_run -o options.xml -f state.sql -e izindo`

2.8 Charge transfer rate

Charge transfer rates can be postulated based on intuitive physical considerations, as it is done in the Gaussian disorder models [22–25]. Alternatively, charge transfer theories can be used to evaluate rates from quantum chemical calculations [1, 8, 20, 26–28]. In spite of being significantly more computationally demanding, the latter approach allows to link the chemical and electronic structure, as well as the morphology, to charge dynamics.

2.8.1 Classical charge transfer rate

The high temperature limit of classical charge transfer theory [29, 30] is often used as a trade-off between theoretical rigor and computational complexity. It captures key parameters which influence charge transport while at the same time providing an analytical expression for the rate. Within this limit, the transfer rate for a charge to hop from a site i to a site j reads

$$\omega_{ij} = \frac{2\pi}{\hbar} \frac{J_{ij}^2}{\sqrt{4\pi\lambda_{ij}k_BT}} \exp\left[-\frac{(\Delta E_{ij} - \lambda_{ij})^2}{4\lambda_{ij}k_BT}\right], \qquad (2.31)$$

where T is the temperature, $\lambda_{ij} = \lambda_{ij}^{int} + \lambda_{ij}^{out}$ is the reorganization energy*, which is a sum of intra- and inter-molecular (outersphere) contributions, ΔE_{ij} is the* site-energy difference*, or driving force, and J_{ij} is the* electronic coupling element*, or transfer integral.*

2.8.2   Semi-classical bimolecular rate

The main assumptions in eq. (2.31) are non-adiabaticity (small electronic coupling and charge transfer
between two diabatic, non-interacting states), and harmonic promoting modes, which are treated classi-
cally. At ambient conditions, however, the intramolecular promoting mode, which roughly corresponds to
C-C bond stretching, has a vibrational energy of $\hbar\omega \approx 0.2\,\mathrm{eV} \gg k_B T$ and should be treated quantum-
mechanically. The outer-sphere (slow) mode has much lower vibrational energy than the intramolecular
promoting mode, and therefore can be treated classically. The weak interaction between molecules also
implies that each molecule has its own, practically independent, set of quantum mechanical degrees of
freedom.

A more general, quantum-classical expression for a bimolecular multi-channel rate is derived in the Sup-
porting Information of ref. [1] and has the following form

$$\omega_{ij} = \frac{2\pi}{\hbar} \frac{|J_{ij}|^2}{\sqrt{4\pi\lambda_{ij}^{out}k_B T}} \sum_{l',m'=0}^{\infty} |\langle\chi_{i0}^c|\chi_{il'}^n\rangle|^2 |\langle\chi_{j0}^n|\chi_{jm'}^c\rangle|^2 \exp\left\{-\frac{\left[\Delta E_{ij} - \hbar(l'\omega_i^n + m'\omega_j^c) - \lambda_{ij}^{out}\right]^2}{4\lambda_{ij}^{out}k_B T}\right\}.$$

$$(2.32) \quad \text{equ:jjortner}$$

If the curvatures of intramolecular PES of charged and neutral states of a molecule are different, that is
$\omega_i^c \neq \omega_i^n$, *the corresponding reorganization energies,* $\lambda_i^{cn} = \frac{1}{2}[\omega_i^n(q_i^n - q_i^c)]^2$ *and* $\lambda_i^{nc} = \frac{1}{2}[\omega_i^c(q_i^n - q_i^c)]^2$,
will also differ. In this case the Franck-Condon (FC) factors for discharging of molecule i read [31]

$$|\langle\chi_{i0}^c|\chi_{il'}^n\rangle|^2 = \frac{2}{2^{l'}l'!} \frac{\sqrt{\omega_i^c\omega_i^n}}{(\omega_i^c + \omega_i^n)} \exp\left(-|s_i|\right) \left[\sum_{\substack{k=0 \\ k\,even}}^{l'} \binom{l'}{k} \left(\frac{2\omega_i^c}{\omega_i^c + \omega_i^n}\right)^{k/2} \frac{k!}{(k/2)!} H_{l'-k}\left(\frac{s_i}{\sqrt{2S_i^{cn}}}\right)\right]^2,$$

$$(2.33)$$

where $H_n(x)$ is a Hermite polynomial, $s_i = 2\sqrt{\lambda_i^{nc}\lambda_i^{cn}}/\hbar(\omega_i^c + \omega_i^n)$, and $S_i^{cn} = \lambda_i^{cn}/\hbar\omega_i^c$. The FC factors
for charging of molecule j can be obtained by substituting $(s_i, S_i^{cn}, \omega_i^c)$ with $(-s_j, S_j^{nc}, \omega_j^n)$. In order to
evaluate the FC factors, the internal reorganization energy λ_i^{cn} can be computed from the intramolecular
PES.

2.8.3   Semi-classical rate

One can also use the quantum-classical rate with a common set of vibrational coordinates [?]

$$\omega_{ij} = \frac{2\pi}{\hbar} \frac{|J_{ij}|^2}{\sqrt{4\pi\lambda_{ij}^{out}k_B T}} \sum_{N=0}^{\infty} \frac{1}{N!} \left(\frac{\lambda_{ij}^{int}}{\hbar\omega^{int}}\right)^N \exp\left(-\frac{\lambda_{ij}^{int}}{\hbar\omega^{int}}\right) \exp\left\{-\frac{\left[\Delta E_{ij} - \hbar N\omega^{int} - \lambda_{ij}^{out}\right]^2}{4\lambda_{ij}^{out}k_B T}\right\}.$$

$$(2.34) \quad \text{equ:jortner}$$

Numerical estimates show that if $\lambda_{ij}^{int} \approx \lambda_{ij}^{out}$ and $|\Delta E_{ij}| \ll \lambda_{ij}^{out}$ the rates are similar to those of eq. (2.31).
In general, there is no robust method to compute λ_{ij}^{out} [32] and both reorganization energies are often
assumed to be of the same order of magnitude. In this case the second condition also holds, unless there
are large differences in electron affinities or ionization potentials of neighboring molecules, e.g. in donor-
acceptor blends.

To calculate rates of the type specified in `options.xml` *for all pairs in the neighbor list and to save them*
into the `state.sql` *file, run the rates calculator. Note that all required ingredients (reorganization*
energies, transfer integrals, and site energies have to be calculated before). `xtp_run -o options.xml`
`-f state.sql -e rates`

2.9 Master equation

sec:kmc

Having determined the list of conjugated segments (hopping sites) and charge transfer rates between them, the next task is to solve the master equation which describes the time evolution of the system

$$\frac{\partial P_\alpha}{\partial t} = \sum_\beta P_\beta \Omega_{\beta\alpha} - \sum_\beta P_\alpha \Omega_{\alpha\beta}, \qquad (2.35)$$

equ:master

where P_α is the probability of the system to be in a state α at time t and $\Omega_{\alpha\beta}$ is the transition rate from state α to state β. A state α is specified by a set of site occupations, $\{\alpha_i\}$, where $\alpha_i = 1(0)$ for an occupied (unoccupied) site i, and the matrix $\hat{\Omega}$ can be constructed from rates ω_{ij}.

The solution of eq. (2.35) is be obtained by using kinetic Monte Carlo (KMC) methods. KMC explicitly simulates the dynamics of charge carriers by constructing a Markov chain in state space and can find both stationary and transient solutions of the master equation. The main advantage of KMC is that only states with a direct link to the current state need to be considered at each step. Since these can be constructed solely from current site occupations, extensions to multiple charge carriers (without the mean-field approximation), site-occupation dependent rates (needed for the explicit treatment of Coulomb interactions), and different types of interacting particles and processes, are straightforward. To optimize memory usage and efficiency, a combination of the variable step size method [33] and the first reaction method is implemented. To obtain the dynamics of charges using KMC, the program `xtp_kmc_run` *executes a specific* calculator *after reading its options (charge carrier type, runtime, numer of carriers etc.) from* `options.xml`.

`xtp_kmc_run -o options.xml -f state.sql -e kmcsingle`
`xtp_kmc_run -o options.xml -f state.sql -e kmcmultiple`

2.9.1 Extrapolation to nondispersive mobilities

sec:nondispersive

Predictions of charge-carrier mobilities in partially disordered semiconductors rely on charge transport simulations in systems which are only several nanometers thick. As a result, simulated charge transport might be dispersive for materials with large energetic disorder [34, 35] and simulated mobilities are system-size dependent. In time-of-flight (TOF) experiments, however, a typical sample thickness is in the micrometer range and transport is often nondispersive. In order to link simulation and experiment, one needs to extract the nondispersive mobility from simulations of small systems, where charge transport is dispersive at room temperature.

Such extrapolation is possible if the temperature dependence of the nondispersive mobility is known in a wide temperature range. For example, one can use analytical results derived for one-dimensional models [36–38]. The mobility-temperature dependence can then be parametrized by simulating charge transport at elevated temperatures, for which transport is nondispersive even for small system sizes. This dependence can then be used to extrapolate to the nondispersive mobility at room temperature [39].

For Alq_3, the charge carrier mobility of a periodic system of 512 molecules was shown to be more than three orders of magnitude higher than the nondispersive mobility of an infinitely large system [39]. Furthermore, it was shown that the transition between the dispersive and nondispersive transport has a logarithmic dependence on the number of hopping sites N. Hence, a brute-force increase of the system size cannot resolve the problem for compounds with large energetic disorder σ, since N increases exponentially with σ^2.

2.10 Macroscopic observables

sec:analysis

Spatial distributions of charge and current densities can provide a better insight in the microscopic mechanisms of charge transport. If O is an observable which has a value O_α in a state α, its ensemble average at time t is a sum over all states weighted by the probability P_α to be in a state α at time t

$$\langle O \rangle = \sum_\alpha O_\alpha P_\alpha. \qquad (2.36)$$

equ:ensemble

If O does not explicitly depend on time, the time evolution of $\langle O \rangle$ can be calculated as

$$\frac{d\langle O \rangle}{dt} = \sum_{\alpha,\beta} \left[P_\beta \Omega_{\beta\alpha} - P_\alpha \Omega_{\alpha\beta} \right] O_\alpha = \sum_{\alpha,\beta} P_\beta \Omega_{\beta\alpha} \left[O_\alpha - O_\beta \right]. \tag{2.37}$$

If averages are obtained from KMC trajectories, $P_\alpha = s_\alpha/s$, where s_α is the number of Markov chains ending in the state α after time t, and s is the total number of chains.

Alternatively, one can calculate time averages by analyzing a single Markov chain. If the total occupation time of the state α is τ_α then

$$\overline{O} = \frac{1}{\tau} \sum_\alpha O_\alpha \tau_\alpha, \tag{2.38}$$

equ:time

where $\tau = \sum_\alpha \tau_\alpha$ is the total time used for time averaging.

For ergodic systems and sufficient sampling times, ensemble and time averages should give identical results. In many cases, the averaging procedure reflects a specific experimental technique. For example, an ensemble average over several KMC trajectories with different starting conditions corresponds to averaging over injected charge carriers in a time-of-flight experiment. In what follows, we focus on the single charge carrier (low concentration of charges) case.

2.10.1   Charge density

sec:occupation

For a specific type of particles, the microscopic charge density of a site i is proportional to the occupation probability of the site, p_i

$$\rho_i = e p_i / V_i, \tag{2.39}$$

where, for an irregular lattice, the effective volume V_i can be obtained from a Voronoi tessellation of space. For reasonably uniform lattices (uniform site densities) this volume is almost independent of the site and a constant volume per cite, $V_i = V/N$, can be assumed. In the macroscopic limit, the charge density can be calculated using a sxtpthing kernel function, i.e. a distance-weighted average over multiple sites. Site occupations p_i can be obtained from eq. (2.36) or eq. (2.38) by using the occupation of site i in state α as an observable.

If the system is in thermodynamic equilibrium, that is without sources or sinks and without circular currents (and therefore no net flux) a condition, known as detailed balance, holds

$$p_j \omega_{ji} = p_i \omega_{ij}, \tag{2.40}$$

equ:detailed_balance

It can be used to test whether the system is ergodic or not by correlating $\log p_i$ and the site energy E_i. Indeed, if $\lambda_{ij} = \lambda_{ji}$ the ratios of forward and backward rates are determined solely by the energetic disorder, $\omega_{ji}/\omega_{ij} = \exp(-\Delta E_{ij}/k_B T)$ (see eq. (2.31)).

2.10.2   Current

sec:vaverage

If the position of the charge, $\vec{r}$, is an observable, the time evolution of its average $\langle \vec{r} \rangle$ is the total current in the system

$$\vec{J} = e \langle \vec{v} \rangle = e \frac{d\langle \vec{r} \rangle}{dt} = e \sum_{i,j} p_j \omega_{ji} (\vec{r}_i - \vec{r}_j). \tag{2.41}$$

equ:current_def

Symmetrizing this expression we obtain

$$\vec{J} = \frac{1}{2} e \sum_{i,j} \left(p_j \omega_{ji} - p_i \omega_{ij} \right) \vec{r}_{ij}, \tag{2.42}$$

equ:current

where $\vec{r}_{ij} = \vec{r}_i - \vec{r}_j$. Symmetrization ensures equal flux splitting between neighboring sites and absence of local average fluxes in equilibrium. It allows to define a local current through site i as

$$\vec{J}_i = \frac{1}{2} e \sum_j \left(p_j \omega_{ji} - p_i \omega_{ij} \right) \vec{r}_{ij}. \tag{2.43}$$

equ:site_current

536 *A large value of the local current indicates that the site contributes considerably to the total current. A*
537 *collection of such sites thus represents most favorable charge pathways [40].*

2.10.3 Mobility and diffusion constant

539 *For a single particle, e.g. a charge or an exciton, a zero-field mobility can be determined by studying particle*
540 *diffusion in the absence of external fields. Using the particle displacement squared, $\Delta \boldsymbol{r}_i^2$, as an observable*
541 *we obtain*

$$2dD_{\gamma\delta} = \frac{d\langle \Delta r_{i,\gamma}\Delta r_{i,\delta}\rangle}{dt} = \sum_{\substack{i,j \\ i\neq j}} p_j\omega_{ji}\left(\Delta r_{i,\gamma}\Delta r_{i,\delta} - \Delta r_{j,\gamma}\Delta r_{j,\delta}\right) = \sum_{\substack{i,j \\ i\neq j}} p_j\omega_{ji}\left(r_{i,\gamma}r_{i,\delta} - r_{j,\gamma}r_{j,\delta}\right).$$

(2.44)

542 *Here $\vec{r}_i$ is the coordinate of the site i, $D_{\gamma\delta}$ is the diffusion tensor, $\gamma, \delta = x, y, z$, and $d = 3$ is the system*
543 *dimension. Using the Einstein relation,*

$$D_{\gamma\delta} = k_B T \mu_{\gamma\delta},$$

(2.45)

544 *one can, in principle, obtain the zero-field mobility tensor $\mu_{\gamma\delta}$. Eq. (2.44), however, does not take into*
545 *account the use of periodic boundary conditions when simulating charge dynamics. In this case, the simu-*
546 *lated occupation probabilities can be compared to the solution of the Smoluchowski equation with periodic*
547 *boundary conditions (see the supporting information for details).*
548 *Alternatively, one can directly analyze time-evolution of the KMC trajectory and obtain the diffusion*
549 *tensor from a linear fit to the mean square displacement, $\overline{\Delta r_{i,\gamma}\Delta r_{i,\delta}} = 2dD_{\gamma\delta}t$.*
550 *The charge carrier mobility tensor, $\hat{\mu}$, for any value of the external field can be determined either from the*
551 *average charge velocity defined in eq. (2.41)*

$$\langle \vec{v}\rangle = \sum_{i,j} p_j\omega_{ji}(\vec{r}_i - \vec{r}_j) = \hat{\mu}\vec{F},$$

(2.46)

552 *or directly from the KMC trajectory. In the latter case the velocity is calculated from the unwrapped (if*
553 *periodic boundary conditions are used) charge displacement vector divided by the total simulation time.*
554 *Projecting this velocity on the direction of the field $\vec{F}$ yields the charge carrier mobility in this particular*
555 *direction. In order to improve statistics, mobilities can be averaged over several KMC trajectories and MD*
556 *snapshots.*

2.10.4 Spatial correlations of energetic disorder

558 *Long-range, e.g. electrostatic and polarization, interactions often result in spatially correlated disor-*
559 *der [41], which affects the onset of the mobility-field (Poole-Frenkel) dependence [36, 42, 43].*
560 *To quantify the degree of correlation, one can calculate the spatial correlation function of E_i and E_j at a*
561 *distance r_{ij}*

$$C(r_{ij}) = \frac{\langle (E_i - \langle E\rangle)(E_j - \langle E\rangle)\rangle}{\langle (E_i - \langle E\rangle)^2\rangle},$$

(2.47)

562 *where $\langle E\rangle$ is the average site energy. $C(r_{ij})$ is zero if E_i and E_j are uncorrelated and 1 if they are fully*
563 *correlated. For a system of randomly oriented point dipoles, the correlation function decays as $1/r$ at large*
564 *distances [44].*
565 *For systems with spatial correlations, variations in site energy differences, ΔE_{ij}, of pairs of molecules from*
566 *the neighbor list are smaller than variations in site energies, E_i, of all individual molecules. Since only*
567 *neighbor list pairs affect transport, the distribution of ΔE_{ij} rather than that of individual site energies,*
568 *E_i, should be used to characterize energetic disorder.*
569 *Note that the* `eanalyze` *calculator takes into account* all *contributions to the site energies* `xtp_run -o`
570 `options.xml -f` `state.sql` `-e` `eanalyze`

Chapter 3

Input and output files

3.1 Atomistic topology

If you are using GROMACS for generating atomistic configurations, it is possible to directly use the topology file provided by GROMACS (`topology.tpr`). In this case the GROMACS residue and atom names should be used to specify the coarse-grained topology and conjugated segments.

A custom topology can also be defined using an XML file. Moreover, it s possible to partially overwrite the information provided in, for example, GROMACS topology file. We will illustrate how to create a custom topology file using DCV2T. The structure of DCV2T, together with atom type definitions, is shown in fig. 3.1. DCV2T has two thiophene (THI) and two dicyanovinyl (NIT) residues. The pdb file which contains residue types, residue numbering, atom names, atom types, and atom coordinates is shown in listing 3.1.
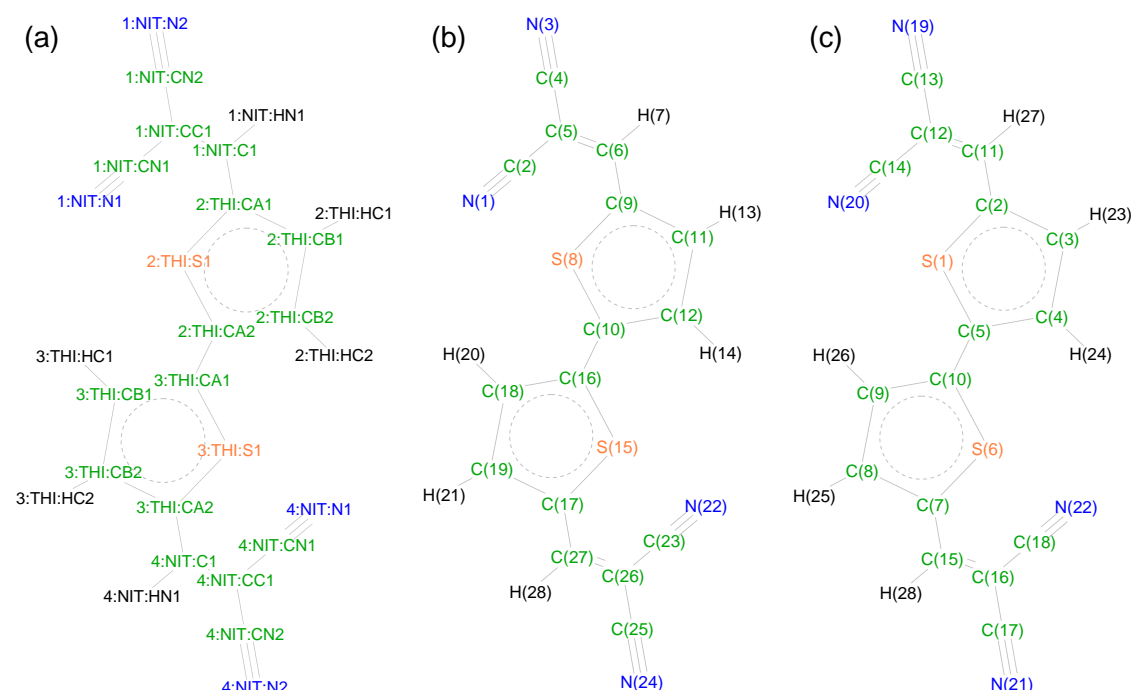

Figure 3.1: (a) DCV2T with atoms labelled according to `residue_number:residue_name:atom_name`. There are four residues and two residue types: thiophene (THI) and dicyanovinyl (NIT). The corresponding pdb file is shown in listing 3.1. Atom numbering is used to split conjugated segments on rigid fragments and to link atomistic ((b) from GROMACS topology) and quantum descriptions (c).

Listing 3.1: pdb file of DCV2T.

```
583
584  HETATM    1  N1   NIT    1      2.388    8.533   11.066   1.00   4.14          N
585  HETATM    2  CN1  NIT    1      1.984    9.553   10.718   1.00   2.54          C
586  HETATM    3  N2   NIT    1     -1.138   10.872   10.087   1.00   3.24          N
587  HETATM    4  CN2  NIT    1      0.003   10.871   10.213   1.00   2.37          C
588  HETATM    5  CC1  NIT    1      1.441   10.824   10.327   1.00   1.91          C
589  HETATM    6  C1   NIT    1      2.193   11.939   10.071   1.00   1.61          C
590  HETATM    7  HN1  NIT    1      1.715   12.710    9.872   1.00   1.97          H
591  HETATM    8  S1   THI    2      4.758   10.743   10.130   1.00   1.52          S
592  HETATM    9  CA1  THI    2      3.613   12.024    9.948   1.00   1.22          C
593  HETATM   10  CA2  THI    2      6.099   11.836    9.997   1.00   1.30          C
594  HETATM   11  CB1  THI    2      4.251   13.243    9.782   1.00   1.39          C
595  HETATM   12  CB2  THI    2      5.658   13.131    9.818   1.00   1.45          C
596  HETATM   13  HC1  THI    2      3.800   14.047    9.660   1.00   1.66          H
597  HETATM   14  HC2  THI    2      6.230   13.860    9.731   1.00   1.74          H
598  HETATM   15  S1   THI    3      8.803   12.414    9.882   1.00   1.38          S
599  HETATM   16  CA1  THI    3      7.456   11.347   10.094   1.00   1.37          C
600  HETATM   17  CA2  THI    3      9.940   11.122   10.152   1.00   1.42          C
601  HETATM   18  CB1  THI    3      7.873   10.048   10.355   1.00   1.73          C
602  HETATM   19  CB2  THI    3      9.267    9.926   10.399   1.00   1.82          C
603  HETATM   20  HC1  THI    3      7.288    9.335   10.487   1.00   2.05          H
604  HETATM   21  HC2  THI    3      9.704    9.123   10.576   1.00   2.21          H
605  HETATM   22  N1   NIT    4     11.235   14.572    9.094   1.00   3.08          N
606  HETATM   23  CN1  NIT    4     11.665   13.566    9.441   1.00   2.04          C
607  HETATM   24  N2   NIT    4     14.733   12.005   10.009   1.00   2.17          N
608  HETATM   25  CN2  NIT    4     13.590   12.149    9.933   1.00   1.77          C
609  HETATM   26  CC1  NIT    4     12.156   12.282    9.861   1.00   1.71          C
610  HETATM   27  C1   NIT    4     11.363   11.220   10.154   1.00   1.59          C
611  HETATM   28  HN1  NIT    4     11.813   10.440   10.389   1.00   1.89          H
612
```

Table 3.1: Description of the XML mapping file (`map.xml`).

topology	Definitions of molecules, segments, and fragments.
molecules	Container for all molecules.
molecule	Mapping of a single molecule.
name	Name of the molecule in the coarse-grained model.
ident	Name (identification) of the molecule in the all-atom representation. This must match the molecule name in the atomistic representation.
segments	Partitioning of the molecule on conjugated segments.
segment	Description of a conjugated segment.
name	Name of a conjugated segment in a molecule.
fragments	Container for all fragments in a segment.
fragment	Description of a rigid fragment.
name	Name of the rigid fragment in a conjugated segment
mdatoms	List of all atoms belonging to the rigid fragment in the format residue number:residue name:atom name.
qmatoms	List of atoms of the rigid fragment in its ground state geometry, atom number:atom type.
weights	Weights are used to determine the fragment center. The order should be the same as in the mdatoms and qmatoms definitions. If the mass of a nucleus in atomic mass units is used, the center of the rigid fragment will be its center of mass.
localframe	Three atoms which define a local frame for each rigid fragment.

3.2 Mapping file

The mapping file (referred here as `map.xml`) is used by the program `xtp_map` to convert an atomistic trajectory to a trajectory with conjugated segments and rigid fragments. This trajectory is stored in a state file and contains positions, names, types of atoms belonging to rigid fragments. The description of the mapping options is given in table 3.1. An example of `map.xml` for a DCV2T molecule is shown in listing 3.2.

The file `map.xml` contains the whole electrostatic information about the molecules as well as the structural information. The toolpdb2map creates a `map.xml` from a pdb file and is a good starting point for further refinement.

Listing 3.2: Examle of `map.xml` for DCV2T. Each rigid fragment (coarse-grained bead) is defined by a list of atoms. Atom numbers, names, and residue names should correspond to those used in `GROMACS` topology (see the corresponding listing 3.1 of the pdb file).

```
<topology> <!-- this file is used to conver an atomistic trajectory to conjugated segments -->
<molecules>
<molecule>
    <name>DCV2T-MOL</name> <!-- name of the conjugated molecule -->
    <mdname>Protein</mdname> <!-- corresponding name of this molecule in the MD trajectory, should be
        the same as the name given at the end of topol.top-->
    <segments>
    <segment>
        <name>DCV</name> <!-- name of the conjugated segment within the molecule -->
        <qmcoords>QC_FILES/DCV2T.xyz</qmcoords>  <!-- QM coordinates of the conjugated segment -->

            <!-- IZINDO INPUT -->
        <basisset>INDO</basisset>
        <orbitals>QC_FILES/DCV2T.orb</orbitals>
        <torbital_h>50</torbital_h><!-- Number of the HOMO Orbital (e.g. alpha electrons, can be
            found in the log-file belonging to DCV2T.orb) -->

            <!-- EMULTIPOLE INPUT -->
        <multipoles_n>MP_FILES/DCV2T.mps</multipoles_n><!-- Multipole file for neutral state -->
        <multipoles_h>MP_FILES/DCV2T_h.mps</multipoles_h><!-- Multipole file for hole state -->
        <map2md>0</map2md><!-- specifies if planar QM coordinates (map2md=0) or MD coordinates (
            map2md=1) of atoms are used for distribution of partial charges. For MD coordinates the
            order and numbering in <mdatoms> and  <mpoles> must be identical it has no impact on the
            qm e.g. DFT or GWBSE calculations-->

                <!-- EINTERNAL INPUT -->
```

```
649         <U_cC_nN_h>0.0</U_cC_nN_h> <!-- Site energy        -->
650         <U_nC_nN_h>0.1</U_nC_nN_h> <!-- Reorg. discharge -->
651         <U_cN_cC_h>0.1</U_cN_cC_h> <!-- Reorg. charge     -->
652
653             <!-- MD QM MP Mapping -->
654         <fragments>
655         <fragment>
656          <name>NI1</name> <!-- name of the rigid fragment within the segment -->
657          <!-- list of atoms in the fragment resnum:resname:atomname -->
658          <mdatoms>1:NIT:N1 1:NIT:CN1 1:NIT:N2  1:NIT:CN2 1:NIT:CC1 1:NIT:C1  1:NIT:HN1</mdatoms>
659          <!-- corresponding ground state geometry atomnumber:atomtype  read from .xyz file-->
660          <qmatoms>  20:N     19:C      14:N      13:C      12:C      11:C      23:H </qmatoms>
661          <!-- corresponding group state geometry multipoles read from .mps files -->
662          <mpoles>  20:N     19:C      14:N      13:C      12:C      11:C      23:H </mpoles>
663          <!-- weights to determine the fragment center (here CoM is used) -->
664          <weights>    14       12       14       12       12       12        1 </weights>
665         <!-- three atoms: define a cartesian local frame, two atoms: fragment is assumed to be
666              rotationally invariant around the axis, one atom: fragment is assumed isotropic -->
667          <localframe> 20 19 14 </localframe>
668         <!-- Optional parameters (if not set <localframe> is used): used when atom labels in the .mps
669              and .xyz file differ or more sites in the .mps file are used, so refers to <mpoles> -->
670          <localframe_mps> 20 19 14 </localframe_mps>
671          <!-- Optional parameters (if not set <localframe> is used):  weights to determine the
672              fragment center (here CoM is used), used when atom labels in the .mps and .xyz file
673              differ or additional sites in the .mps file are used -->
674         <weights_mps>     14       12       14       12       12       12        1 </
675             weights_mps>
676         <!-- Optional flag: says  if a site is virtual or not, (virtual=1, real=0)-->
677         <virtual_mps>     0        0        0        0        0        0        0 </
678             virtual_mps>
679        </fragment>
680
681      <fragment>
682         <name>TH1</name>
683         <mdatoms>2:THI:S1 2:THI:CA1 2:THI:CA2 2:THI:CB1 2:THI:CB2 2:THI:HC1 2:THI:HC2</mdatoms>
684         <qmatoms>   7:S      8:C       6:C       9:C      10:C      24:H     25:H </qmatoms>
685         <mpoles>    7:S      8:C       6:C       9:C      10:C      24:H     25:H </mpoles>
686         <weights>    32       12       12       12       12        1        1 </weights>
687         <localframe> 7 8 6 </localframe>
688      </fragment>
689
690      <fragment>
691         <name>TH2</name>
692         <mdatoms>3:THI:S1 3:THI:CA1 3:THI:CA2 3:THI:CB1 3:THI:CB2 3:THI:HC1 3:THI:HC2</mdatoms>
693         <qmatoms>   3:S      4:C       2:C       5:C       1:C      26:H     27:H </qmatoms>
694         <weights>    32       12       12       12       12        1        1 </weights>
695         <localframe> 3 4 2 </localframe>
696      </fragment>
697
698      <fragment>
699         <name>NI2</name>
700         <mdatoms>4:NIT:N1 4:NIT:CN1 4:NIT:N2  4:NIT:CN2 4:NIT:CC1 4:NIT:C1  4:NIT:HN1</mdatoms>
701         <qmatoms>  22:N     21:C      18:N      17:C      16:C      15:C      28:H </qmatoms>
702         <mpoles>   22:N     21:C      18:N      17:C      16:C      15:C      28:H </mpoles>
703         <weights>    14       12       14       12       12       12        1 </weights>
704         <localframe> 22 21 18 </localframe>
705      </fragment>
706      </fragments>
707
708    </segments>
709 </molecule>
710 </molecules>
711 </topology>
712
```

3.3   Molecular orbitals

If the semi-empirical method is used to calculate electronic coupling elements, molecular orbitals of all molecules must be supplied. They can be generated using Gaussian *program. The* Gaussian *input file for DCV2T is shown in listing 3.3. Provided with this input,* Gaussian *will generate* fort.7 *file which contains the molecular orbitals of a DCV2T. This file can be renamed to* DCV2T.orb. *Note that the order of the atoms in the input file and the order of coefficients should always match. Therefore, the coordinate part of the input file must be supplied together with the orbitals. We will assume the coordinates, in the format* atom_type: x y z, *is saved to the* DCV2T.xyz *file.*

Izindo requires the specification of orbitals for hole and electron transport in `map.xml`*. They are the HOMO and LUMO respectively and can be retrieved from the* `log` *file from which the* `DCV2T.orb` *file is generated. The number of* `alpha electrons` *is the HOMO, the LUMO is HOMO+1*

list:zindo_orbitals

Listing 3.3: `Gaussian` input file `get_orbitals.com` used for generating molecular orbitals. The first line contains the name of the check file, the second the requested RAM. `int=zindos` requests the method ZINDO, `punch=mo` states that the molecular orbitals ought to be written to the `fort.7` file, `nosymm` forbids use of symmetry and is necessary to ensure correct position of orbitals with respect to the provided coordinates. The two integer numbers correspond to the charge and multiplicity of the system: 0 1 corresponds to a neutral system with a multiplicity of one. They are followed by the types and coordinates of all atoms in the molecule.

```
%chk=DCV2T.chk
%mem=100Mb
#p int=zindos punch=mo nosymm

DCV2T molecular orbitals

0 1
S          -1.44650         2.12185         0.00135
C          -2.43098         0.58936        -0.00048
C          -1.59065        -0.51859        -0.00146
C          -0.21222        -0.22233        -0.00095
C           0.07761         1.13376         0.00040
S           2.87651         0.79316         0.00148
C           3.86099         2.32565         0.00235
C           3.02066         3.43359         0.00231
C           1.64223         3.13733         0.00162
C           1.35240         1.78125         0.00114
C          -3.85350         0.52245        -0.00081
C          -4.79569         1.52479        -0.00008
C          -6.18500         1.18622        -0.00117
C          -4.47544         2.91565         0.00081
C           5.28350         2.39256         0.00296
C           6.22569         1.39020         0.00327
C           7.61500         1.72876         0.00432
C           5.90542        -0.00064         0.00333
N          -7.32389         0.89743        -0.00195
N          -4.21872         4.06274         0.00142
N           8.75389         2.01754         0.00510
N           5.64864        -1.14772         0.00361
H          -1.98064        -1.52966        -0.00256
H           0.55785        -0.98374        -0.00169
H           3.41065         4.44466         0.00272
H           0.87216         3.89874         0.00147
H          -4.24640        -0.49192        -0.00188
H           5.67641         3.40692         0.00337
```

3.4 Monomer calculations for DFT transfer integrals

list:edft_gaussian_xml

Listing 3.4: Example `package.xml` file for the `Gaussian` package required in the options of the `edft calculator` for the monomer calculations as preparation for the determination of transfer integrals using DIPRO.

```
<package>
  <name>gaussian</name>
  <executable>g09</executable>
  <checkpoint></checkpoint>
  <scratch></scratch>

  <charge>0</charge>
  <spin>1</spin>
  <options># pop=minimal pbepbe/6-311g** scf=tight punch=mo nosymm test</options>
```

```
772    <memory>1Gb</memory>
773    <threads>2</threads>
774
775    <cleanup></cleanup>
776  </package>
```

Listing 3.5: Example `package.xml` file for the `Turbomole` package required in the options of the edft calculator for the monomer calculations as preparation for the determination of transfer integrals using DIPRO.

```
778
779  <package>
780    <name>turbomole</name>
781    <executable>ridft</executable>
782    <scratch>/tmp</scratch>
783
784    <options>
785  TITLE
786  a coord
787  *
788  no
789  b all def-TZVP
790  *
791  eht
792  y
793  0
794  y
795  dft
796  on
797  func
798  pbe
799  grid
800  m3
801  *
802  ri
803  on
804  m 300
805  *
806  scf
807  conv
808  7
809  iter
810  200
811
812  marij
813
814  q
815    </options>
816
817    <cleanup></cleanup>
818  </package>
```

Listing 3.6: Example `package.xml` file for the `NWChem` package required in the options of the edft calculator for the monomer calculations as preparation for the determination of transfer integrals using DIPRO.

```
820
821  <package>
822    <name>nwchem</name>
823    <executable>nwchem</executable>
824    <checkpoint></checkpoint>
825    <scratch>/tmp/nwchem</scratch>
826    <charge>0</charge>
827    <spin>1</spin>
828    <threads>1</threads>
829    <memory></memory>
830    <options>
831  start
```

```
832  basis
833   * library 6-311gss
834  end
835  memory 1500 mb
836
837  dft
838   xc xpbe96 cpbe96
839   direct
840   iterations 100
841   noprint "final vectors analysis"
842  end
843  task dft
844  </options>
845    <cleanup></cleanup>
846
847  </package>
```

3.5 Pair calculations for DFT transfer integrals

Listing 3.7: Example `package.xml` file for the `Gaussian` package required in the options of the `idft` calculator for the pair calculations and the determination of transfer integrals using `DIPRO`.

```
850  <package>
851    <name>gaussian</name>
852    <executable>g09</executable>
853    <checkpoint></checkpoint>
854    <scratch></scratch>
855
856    <charge>0</charge>
857    <spin>1</spin>
858    <options># pop=minimal pbepbe/6-311g** nosymm  IOp(3/33=1,3/36=-1) punch=mo guess=cards scf=(maxcycle=1,
859    <memory>1Gb</memory>
860    <threads>1</threads>
861
862    <cleanup></cleanup>
863
864  </package>
```

Listing 3.8: Example `package.xml` file for the `Turbomole` package required in the options of the `idft` calculator for the pair calculations and the determination of transfer integrals using `DIPRO`.

```
866  <package>
867    <name>turbomole</name>
868    <executable>ridft</executable>
869    <scratch>/tmp</scratch>
870
871    <options>
872  $intsdebug cao
873  a coord
874  *
875  no
876  b all def-TZVP
877  *
878  eht
879  y
880  0
881  y
882  dft
883  on
884  func
885  pbe
886  grid
887  m3
888  *
889  ri
890  on
```

```
891   m 300
892   *
893   scf
894   conv
895   7
896   iter
897   1
898   diis
899   3
900   damp
901   0.00
902
903
904
905   marij
906
907   q
908     </options>
909
910     <cleanup></cleanup>
911
912   </package>
```

Listing 3.9: Example `package.xml` file for the `NWChem` package required in the options of the `idft calculator` for the pair calculations and the determination of transfer integrals using `DIPRO`.

```
913
914   <package>
915     <name>nwchem</name>
916     <executable>nwchem</executable>
917     <checkpoint></checkpoint>
918     <scratch>/tmp/nwchem</scratch>
919     <charge>0</charge>
920     <spin>1</spin>
921     <memory></memory>
922     <threads>1</threads>
923     <options>
924   start
925   basis
926    * library 6-311gss
927   end
928   memory 1500 mb
929
930   dft
931    print "ao overlap"
932    xc xpbe96 cpbe96
933    direct
934    iterations 1
935    convergence nodamping nodiis
936    noprint "final vectors analysis"
937    vectors input system.movecs
938   end
939   task dft
940   </options>
941     <cleanup></cleanup>
942
943   </package>
```

3.6 DFT transfer integrals

Listing 3.10: Example `TI.xml` file created as the output of a `DIPRO` calculation. Due to slightly different implementations, the orbitals indices refer to monomer indices in a `Gaussian` run but to indices in the merged dimer guess in a `Turbomole` run.

```
945
946   <pair name="pair_100_155">
947       <parameters>
948           <HOMO_A>162</HOMO_A>
```

```
949         <NoccA>1</NoccA>
950         <LUMO_A>164</LUMO_A>
951         <NvirtA>1</NvirtA>
952         <HOMO_B>161</HOMO_B>
953         <NoccB>1</NoccB>
954         <LUMO_B>163</LUMO_B>
955         <NvirtB>1</NvirtB>
956     </parameters>
957     <transport name="hole">
958         <channel name="single">
959             <J>1.546400416750696E-003</J>
960             <e_A>-6.30726450715697</e_A>
961             <e_B>-6.36775613794166</e_B>
962         </channel>
963         <channel name="multi">
964             <molecule name="A">
965                 <e_HOMOm0>-6.30726450715697</e_HOMOm0>
966             </molecule>
967             <molecule name="B">
968                 <e_HOMOm0>-6.36775613794166</e_HOMOm0>
969             </molecule>
970                 <dimer name="integrals">
971                     <T_00>1.546400416750696E-003</T_00>
972                     <J_sq_degen>2.391354248926727E-006</J_sq_degen>
973                     <J_sq_boltz>2.391354248926727E-006</J_sq_boltz>
974                 </dimer>
975         </channel>
976     </transport>
977     <transport name="electron">
978         <channel name="single">
979             <J>-2.797473760331286E-003</J>
980             <e_A>-4.50318366770689</e_A>
981             <e_B>-4.53143397059021</e_B>
982         </channel>
983         <channel name="multi">
984             <molecule name="A">
985                 <e_LUMOp0>-4.50318366770689</e_LUMOp0>
986             </molecule>
987             <molecule name="B">
988                 <e_LUMOp0>-4.53143397059021</e_LUMOp0>
989             </molecule>
990                 <dimer name="integrals">
991                     <T_00>-2.797473760331286E-003</T_00>
992                     <J_sq_degen>7.825859439742066E-006</J_sq_degen>
993                     <J_sq_boltz>7.825859439742066E-006</J_sq_boltz>
994                 </dimer>
995         </channel>
996     </transport>
997 </pair>
998
```

3.7 State file

All data structures are saved to the `state.sql` *file in sqlite3 format, see http://www.sqlite.org/. They are available in form of tables in the* `state.sql` *file as can be seen by the command*

`sqlite3` `state.sql` `" .tables "`

An example of such a table are `molecules`*. The full table can be displayed using the command (similar for the other tables)*

`sqlite3` `state.sql` `" SELECT * FROM molecules "`

The meaning of all the entries in the table can be displayed by a command like

`sqlite3` `state.sql` `" .SCHEMA molecules "`

The first and second entry are integers for internal and regular id of the molecule and the third entry is the name. A single field from the table like the name of the molecule can be displayed by a command like

1010 `sqlite3 state.sql " SELECT name FROM molecules "`

1011 *Besides* `molecules`, *the following tables are stored in the* `state.sql`:

1012 `conjseg_properties:`

1013 *Conjugated segments are stored with id, name and x,y,z coordinates of the center of mass in nm.*

1014 `conjsegs:`

1015 *Reorganization energies for charging or discharging a conjugated segment are stored together with the*

1016 *coulomb energy and any other user defined energy contribution (in eV) and occupation probabilities.*

1017 `pairs:`

1018 *The pairs from the neighborlist are stored with the pair id, the id of the first and second segment, the rate*

1019 *from the first to the second , the rate from the second to the first (both in* $s^{-}1$*) and the x,y,z coordinates in*

1020 *nm of the distance between the first and the second segment.*

1021 `pairintegrals:`

1022 *Transfer integrals for all pairs are stored in the following way: The pair id , the number for counting*

1023 *possible different electronic overlaps (e.g if only the frontier orbitals are taken into account this is always*

1024 *zero, while an effective value is stored in addition to the different overlaps of e.g. HOMO-1 and HOMO-1*

1025 *if more frontier orbitals are taken into account) and the integral in eV.*

1026 `pairproperties:`

1027 *The outer sphere reorganization energy of all pairs is stored by an id, the pair id, a string* `lambda_outer`

1028 *and the energy in eV.*

1029 `conjsegs:`

1030 *Conjugated segments are saved in the following way: The id, the name, the type, the molecule id, the time*

1031 *frame, the x,y,z coordinates in nm and the occupation probability.*

1032 `conjseg_properties:`

1033 *Properties of the conjugated segments like reorganization energies for charging or discharging a charge*

1034 *unit or the coulomb contribution to the site energy are stored by: id, conjugated segment id, a string like*

1035 `lambda_intra_charging, lambda_intra_discharging` *or* `energy_coulomb` *and a corre-*

1036 *sponding value in eV.*

1037 *The tables* `rigidfrag_properties`, `rigidfrags` *and* `frames` *offer information about rigid frag-*

1038 *ments and time frames including periodic boundary conditions.*

1039 *The data in the* `state.sql` *file can also be modified by the user. Here is an example how to modify*

1040 *the transfer integral between the conjugated segments number one and two assuming that they are in the*

1041 *neighborlist. Their pair id can be found by the command*

1042 `pair_ID='sqlite3 state.sql "SELECT _id FROM pairs WHERE conjseg1=1 AND conjseg2=2"'`

1043 *The old value of the transfer integral can be deleted using*

1044 `sqlite3 state.sql "DELETE FROM pair_integrals WHERE pair=$pair_ID"`

1045 *Finally the new transfer integral J can be written to the* `state.sql` *file by the command*

1046 `sqlite3 state.sql "INSERT INTO pair_integrals (pair,num,J) VALUES ($pair_ID,0,$J)"`

1047 *Here the num=0 indicates that only the effective transfer integrals is written to the file, while other values*

1048 *of num would correspond to overlap between other orbitals than the frontier orbitals.*

1049 *In a similar way the coulomb contribution to the site energy of the first conjugated segment can be over-*

1050 *written by first getting its id*

1051 `c_ID='sqlite3 state.sql "SELECT _id from conjseg_properties  where conjseg=1 AND`

1052 `key =\"energy_coulomb\""`

1053 *Then deleting the old value*

1054 `sqlite3 state.sql "DELETE FROM from conjseg_properties WHERE _id=$c_ID"`

1055 *Then the new coulomb energy E can be written to this id*

1056 `sqlite3 state.sql "INSERT INTO conjseg_properties (_id,conjseg,key,value)`

1057 `VALUES ($c_ID,1,\"energy_coulomb\",$E)"`

1058 *Finally the resulting coulomb contribution to all conjugated segments can be displayed by*

1059 `sqlite3 state.sql "SELECT * from conjseg_properties WHERE key=\"energy_coulomb\""`

1060

Chapter 4

Reference

4.1 Programs

Programs execute specific tasks (calculators).

4.1.1 xtp_testsuite

Performs tests en suite + optional arguments:

$-h$, $--help$ *show this help message and exit*

$-e$ [[...]], $--execute$ [[...]] *Tests to perform, accepts regex (def=".*")*

$-l$, $--listonly$ *List all tests available, then quit.*

$-x$, $--xml$ *Test-suite file (def="\$VOTCASHARE/xtp/xml/testsuite.xml")*

$-s$, $--source$ *Test source input directory (def="source")*

$-td$, $--testdirectory$ *Test run directory (def="suite")*

$-t$, $--target$ *Directory where to store targets (def="targets")*

$-r$, $--reference$ *Folder with reference data to compare to (def="reference")*

$-g$, $--generate$ *Generate reference from targets (def=False)*

$-cmp$, $--compareonly$ *Only compare existing targets to reference (def=False)*

$-v$, $--verbose$ *The wordy version (def=False)*

$-sh$, $--showoutput$ *Display VOTCA::XTP exec. output (def=False)*

$-c$, $--clean$ *To clean or not to clean test dir. (def=False)*

$-m$, $--mailto$ *Mail the result. (def=False)*

4.1.2 xtp_update

Updates the state file + optional arguments:

$-h$, $--help$ *show this help message and exit*

$-f$ SQLFILE, $--file$ SQLFILE *State file to update.*

4.1.3 xtp_update_exciton

Updates the state file for singlets and triplets + optional arguments:

$-h$, $--help$ *show this help message and exit*

$-f$ SQLFILE, $--file$ SQLFILE *State file to update.*

4.1.4 xtp_basisset

xtp_update, version 1.4-dev gitid: ad1d776 Creates votca xml basissetfiles from NWCHEM basissetfiles

optional arguments:

1092   *-h, --help show this help message and exit*

1093   *-f NWCHEM, --inputnw NWCHEM NWchem file containing the basisset.*

1094   *-o OUTPUTFILE, --outputvotca OUTPUTFILE Path of votca outputfile*

4.1.5   xtp_map

prog:xtp_map

1096   *Generates QM|MD topology*

1097   *-h [--help] display this help and exit*

1098   *-v [--verbose] be loud and noisy*

1099   *-t [--topology] arg topology*

1100   *-c [--coordinates] arg coordinates or trajectory*

1101   *-s [--segments] arg definition of segments and fragments*

1102   *-f [--file] arg state file*

4.1.6   xtp_run

prog:xtp_run

1104   *Runs excitation/charge transport calculators*

1105   *-h [--help] display this help and exit*

1106   *-v [--verbose] be loud and noisy*

1107   *-o [--options] arg calculator options*

1108   *-f [--file] arg sqlight state file, *.sql*

1109   *-i [--first-frame] arg (=1) start from this frame*

1110   *-n [--nframes] arg (=1) number of frames to process*

1111   *-t [--nthreads] arg (=1) number of threads to create*

1112   *-s [--save] arg (=1) whether or not to save changes to state file*

1113   *-e [--execute] arg List of calculators separated by ',' or ' '*

1114   *-l [--list] Lists all available calculators -d [--description] arg Short description of a cal-*

1115   *culator*

4.1.7   xtp_tools

prog:xtp_tools

1117   *Runs excitation/charge transport tools*

1118   *-h [--help] display this help and exit*

1119   *-v [--verbose] be loud and noisy*

1120   *-t [--nthreads] arg (=1) number of threads to create*

1121   *-o [--options] arg calculator options Tools:*

1122   *-e [--execute] arg List of tools separated by ',' or ' '*

1123   *-l [--list] Lists all available tools -d [--description] arg Short description of a tool*

4.1.8   xtp_parallel

prog:xtp_parallel

1125   *Runs job-based heavy-duty calculators*

1126   *-h [--help] display this help and exit*

1127   *-v [--verbose] be loud and noisy*

1128   *-o [--options] arg calculator options*

1129   *-f [--file] arg sqlite state file, *.sql*

1130   *-i [--first-frame] arg (=1) start from this frame*

1131   *-n [--nframes] arg (=1) number of frames to process*

1132   *-t [--nthreads] arg (=1) number of threads to create*

1133   *-s [--save] arg (=1) whether or not to save changes to state file*

1134   *-r [--restart] arg restart pattern: 'host(pc1:234) stat(FAILED)'*

1135   *-c [--cache] arg (=8) assigns jobs in blocks of this size*

1136   *-j [--jobs] arg (=run) task(s) to perform: input, run, import*

1137 `-m [ --maxjobs ] arg (=-1)` *maximum number of jobs to process (-1 = inf)*
1138 `-e [ --execute ] arg` *List of calculators separated by ',' or ' '*
1139 `-l [ --list ]` *Lists all available calculators* `-d [ --description ] arg` *Short description of a cal-*
1140 *culator*

4.1.9 xtp_dump

1141

1142 *Extracts information from the state file*
1143 `-h [ --help ]` *display this help and exit*
1144 `-v [ --verbose ]` *be loud and noisy*
1145 `-o [ --options ] arg` *calculator options*
1146 `-f [ --file ] arg` *sqlight state file, *.sql*
1147 `-i [ --first-frame ] arg (=1)` *start from this frame*
1148 `-n [ --nframes ] arg (=1)` *number of frames to process*
1149 `-t [ --nthreads ] arg (=1)` *number of threads to create*
1150 `-s [ --save ] arg (=1)` *whether or not to save changes to state file Extractors:*
1151 `-e [ --extract ] arg` *List of extractors separated by ',' or ' '*
1152 `-l [ --list ]` *Lists all available extractors* `-d [ --description ] arg` *Short description of an ex-*
1153 *tractor*

4.1.10 xtp_overlap

1154

1155 *moo_overlap*
1156 `-h [ --help ]` *display this help and exit*
1157 `-v [ --verbose ]` *be loud and noisy MOO Options:*
1158 `--conjseg arg` *xml file describing two conjugated segments*
1159 `--pos1 arg` *position and orientation of molecule 1*
1160 `--pos2 arg` *position and orientation of molecule 2*
1161 `--pdb arg (=geometry.pdb)` *pdb file of two molecules*

4.1.11 xtp_kmc_run

1162

1163 *kmc_run, version 1.4-dev gitid: ad1d776 (compiled Sep 15 2016, 05:52:11) Runs specified calculators*
1164 `-h [ --help ]` *display this help and exit*
1165 `-v [ --verbose ]` *be loud and noisy*
1166 `-o [ --options ] arg` *program and calculator options*
1167 `-f [ --file ] arg` *sqlite state file*
1168 `-t [ --textfile ] arg` *output text file (otherwise: screen output)*
1169 `-e [ --execute ] arg` *list of calculators separated by commas or spaces*
1170 `-l [ --list ]` *lists all available calculators* `-d [ --description ] arg` *detailed description of a*
1171 *calculator*

4.2 Calculators

1172

1173 *Calculator is a piece of code which computes specific system properties, such as site energies, transfer*
1174 *integrals, etc.* `xtp_run`, `xtp_kmc_run` *are wrapper programs which executes such calculators. The*
1175 *generic syntax is*

1176 `xtp_run -e "calc1, calc2, ..." -o options.xml`

1177 *File* `options.xml` *lists all options needed to run a specific calculator. The format of this file is explained*
1178 *in listing 4.1. A complete list of calculators is given in the calculators reference section.*

Listing 4.1: A part of the `options.xml` file with options for the `calculator_name{1,2}` calculators.

```
<calculator_name1>
        <option1>value1</option1>
        <option2>value2</option2>
        ...
</calculator_name1>

<calculator_name2>
        <option1>value1</option1>
        <option2>value2</option2>
        ...
</calculator_name2>
...
```

A list of all calculators and their short descriptions can be obtain using

`xtp_run --list`

A detailed description of all options of a specific calculator(s) is available via

`xtp_run --desc calc1,calc2,...`

4.2.1 coupling

Electronic couplings from log and orbital files (GAUSSAIN, TURBOMOLE, NWChem)

option	default	unit	description
package			First-principles package
output	coupling.out.xml		Output file
degeneracy	0	eV	Criterium for the degeneracy of two levels
moleculeA			
log	A.log		Log file of molecule A
orbitals	A.orb		Orbitals file
levels	3		Output HOMO, ..., HOMO-levels; LUMO, ..., LUMO+levels
trim	2		
moleculeB			
log	B.log		Log file of molecule B
orbitals	B.orb		Orbitals file
levels	3		Output HOMO, ..., HOMO-levels; LUMO, ..., LUMO+levels
trim	2		
dimerAB			
log	AB.log		Log file of dimer AB
orbitals	A.orb		Orbitals file

Return to the description of `coupling`.

4.2.2 excitoncoupling

Exciton couplings from serialized orbital files

option	default	unit	description
output	excitoncoupling.c		Output file
bsecoupling			
orbitalsA	A.orb		Serialized orbitals file
orbitalsB	B.orb		Serialized orbitals file
orbitalsAB	AB.orb		Serialized orbitals file

Return to the description of `excitoncoupling`.

1203 **4.2.3 gencube**

calc:gencube

1204 *Tool to generate cube files from .orb file*

option	default	unit	description
output	state.cube		Output file
input	system.orb		Input file
padding	6.5		How far the grid should start from the molecule
xsteps	25		Gridpoints in x-direction
ysteps	25		Gridpoints in y-direction
zsteps	25		Gridpoints in z-direction
state	1		State to generate cube file for
spin			Singlet or Triplet
type	ground		qp:quasiparticle,ground:groundstate,transition:transitionstate,excited/excited-gs:excitedstate density/density excited-ground state
mode	new		new: generate new cube file, substract: substract to cube files specified below
infile1			Cubefile to substract infile2 from
infile2			Cubefile to substract from infile1

1205 *Return to the description of* `gencube`.

1206 **4.2.4 log2mps**

calc:log2mps

1207 *Generates an mps-file (with polar-site definitions) from a QM log-file*

option	default	unit	description
package			QM package
logfile			Log-file generated by QM package, with population/esp-fit data

1208 *Return to the description of* `log2mps`.

1209 **4.2.5 molpol**

calc:molpol

1210 *Molecular polarizability calculator (and optimizer)*

option	default	unit	description
mpsfiles			
input			mps input file
output			mps output file
polar			xml file with infos on polarizability tensor
induction			
expdamp			Thole sharpness parameter
wSOR			mixing factor for convergence
maxiter			maximum number of iterations
tolerance			rel. tolerance for induced moments
target			
optimize			if 'true', refine atomic polarizabilities to match molecular polarizable volume specified in target.molpol
molpol			target polarizability tensor in format xx xy xz yy yz zz (this should be in the eigen-frame, hence xy = xz = yz = 0), if optimize=true the associated polarizable volume will be matched iteratively and the resulting set of polar sites written to mps-files.output
tolerance			relative tolerance when optimizing the polarizable volume

1211 *Return to the description of* `molpol`.

4.2.6   orb2isogwa

Analysis tool for QM results stores in serialized file

option	default	unit	description
output	qmanalyze.out		Output file
property			
input	molecule.orb		Serialized file

Return to the description of `orb2isogwa`.

4.2.7   partialcharges

Tool to derive partial charges from QM results stores in serialized file

option	default	unit	description
output	Moleculecharges.		Output file either .mps or .pdb
input	molecule.orb		Serialized file
esp2multipole			options for the method

Return to the description of `partialcharges`.

4.2.8   pdb2map

Converts MD + QM files to VOTCA mapping. Combinations: pdb+xyz,gro+xyz,pdb

option	default	unit	description
pdb	conf.pdb		Input pdb file
gro	conf.gro		Input gro file
xyz	conf.xyz		Input xyz file
xml	conf.xml		Resulting xml file

Return to the description of `pdb2map`.

4.2.9   pdb2top

Generates fake Gromacs topology file .top

option	default	unit	description
num	1		Num of mols in the box
pdb	conf.pdb		Input pdb file
gro	conf.gro		Input gro file

Return to the description of `pdb2top`.

4.2.10   ptopreader

Reads binary .ptop-files (serialized from ewdbgpol) and processes them into something readable

option	default	unit	description
ptop_file			Binary archive .ptop-file

Return to the description of `ptopreader`.

4.2.11 qmanalyze

Analysis tool for QM results stores in serialized file

option	default	unit	description
output	qmanalyze.out		Output file
BSE			additonal info about BSE results
input	molecule.orb		Serialized file

Return to the description of `qmanalyze`*.*

4.2.12 eanalyze

Histogram and correlation function of site energies and pair energy differences

option	default	unit	description
resolution_sites		eV	Bin size for site energy histogram
resolution_pairs		eV	Bin size for pair energy histogram
resolution_space		eV	Bin size for site energy correlation
states			?

Return to the description of `eanalyze`*.*

4.2.13 eimport

Imports site energies from the output file of emultipole and writes them to the state file

option	default	unit	description

Return to the description of `eimport`*.*

4.2.14 einternal

Reads in site and reorganosation energies and writes them to the state file

option	default	unit	description
energiesXML			XML input file with vacuum site, reorganization (charging, discharging) energies

Return to the description of `einternal`*.*

4.2.15 emultipole

Evaluates polarization contribution based on the Thole model

option	default	unit	description
multipoles			Polar Site Definitions in GDMA punch-file format
control			Control options for induction computation
induce	1		Enter '1' / '0' to toggle induction on / off
first			First segment for which to compute site energies
last			Last segment for which to compute site energies
output			File to write site energies to. Site energies are also stored in the state file
check			Check mapping of polar sites to fragment
tholeparam			Thole parameters required for charge-smearing
cutoff		nm	Cut-off beyond which all interactions are neglected

cutoff2		nm	Cut-off beyond which polarization is neglected
expdamp			Damping exponent used in exponential damping function
scaling			1-n interaction scaling, currently not in use
esp			Control options for potential calculation
calcESP			Enter '1' / '0' to toggle on / off. If '1', site energies will not be evaluated
cube			
grid			XYZ file specifying grid points for potential evaluation
output			File to write grid-point potential to
esf			Control options for field calculation
calcESF			Enter '1' / '0' to toggle on / off. If '1', site energies will not be evaluated
grid			XYZ file specifying grid points for field evaluation
output			File to write grid-point field to
alphamol			Control options for molecular-polarizability calculation
calcAlpha			Enter '1' / '0' to toggle on / off. If '1', site energies will not be evaluated
output			File to write polarizability tensor in global frame and in diagonal form to
convparam			Convergence parameters for self-consistent field calculation
wSOR_N			Mixing factor for successive overrelaxation of neutral system, usually between 0.3 and 0.5
wSOR_C			Mixing factor for successive overrelaxation of charged system, usually between 0.3 and 0.5
tolerance			Convergence criterion, fulfilled if relative change smaller than tolerance
maxiter			Maximum number of iterations in the convergence loop

Return to the description of `emultipole`.

4.2.16 eoutersphere

Evaluates outersphere reorganization energy

option	default	unit	description
multipoles			XML allocation polar sites
method			Type of the method: **constant** - all pairs have value **lambda**. **spheres** - molecules are treated as spheres with radii **radius** and Pekar factor **pekar**. **dielectric** - with Pekar factor **pekar** and partial charges from resulting dielectric fields
lambdaconst		eV	The value for all pairs in the **constant** method
pekar			Pekar factor used for methods **spheres** and **dielectric**
segment			
type			
radius			
segment			
type			
radius			
cutoff		nm	Cutoff radius in between pair and the exterior molecule. Can be used in **spheres** and **dielectric**

Return to the description of `eoutersphere`.

4.2.17 ianalyze

Evaluates a histogram of a logarithm of squared couplings

option	default	unit	description
resolution_logJ2			Bin size of histogram log(J2)
resolution_space		nm	Bin size for r in log(J2(r))
states			States for which to calculate the histogram. Example: 1 -1

Return to the description of `ianalyze`.

4.2.18 iimport

calc:iimport

Imports electronic couplings from xml of xtp-dipro using folders of pairdump

option	default	unit	description
idft_jobs_file			idft jobs file
probabilityfile_h	ianalyze.ispatial-h.out		For coarse grained simulations provide here the distance dependent means and sigmas of hole transfer integrals. This file can be created using the ianalyze calculator.
probabilityfile_e	ianalyze.ispatial-e.out		For coarse grained simulations provide here the distance dependent means and sigmas of electron transfer integrals. This file can be created using the ianalyze calculator.

Return to the description of `iimport`.

4.2.19 izindo

calc:izindo

Semiempirical electronic coupling elements for all neighbor list pairs

option	default	unit	description
orbitalsXML			File with paths to .orb files

Return to the description of `izindo`.

4.2.20 jobwriter

calc:jobwriter

Writes list of jobs for a parallel execusion

option	default	unit	description
keys			job type
single_id			Segment ID as argument for mps.single
kmc_cutoff		nm	Pair-interaction cut-off as argument for mps.kmc

Return to the description of `jobwriter`.

4.2.21 pairdump

calc:pairdump

Coordinates of molecules and pairs from the neighbor list

option	default	unit	description
molecules			If **true** outputs single molecules, otherwise only pairs

Return to the description of `pairdump`.

4.2.22 panalyze

calc:panalyze

Probability of neighbours being in the pair list as a function of their centre of mass distance

option	default	unit	description
resolution_space		nm	Spatial resolution for the probability function.

Return to the description of `panalyze`.

4.2.23   profile

Density and site energy profiles

option	default	unit	description
axis			Axis along which to calculate density and energy profiles
direction	0 0 1		Axis direction
min		nm	Minimal projected position for manual binning
max		nm	Maximal projected position for manual binning
bin	0.1	nm	Spatial resolution of the profile
auto	1		'0' for manual binning using min and max, '1' for automated
particles			
type	segments		What centers of mass to use: 'segments' or 'atoms'
first	1		ID of the first segment
last	-1		ID of the last segment, -1 is the list end
output			
density	density.dat		Density profile file
energy	energy.dat		Energy profile file

Return to the description of `profile`.

4.2.24   rates

Hopping rates using classical or semi-classical expression

option	default	unit	description
field			Field in x y z direction
temperature		K	Temperature for rates
method			Method chosen to compute rates. Can either be **marcus** or **jortner**. The first is the high temperature limit of Marcus theory, the second is the rate proposed by Jortner and Bixon
nmaxvib	20		If the method of choice is **jortner**, the maximal number of excited vibrations on the molecules has to be specified as an integer for the summation
omegavib	0.2	eV	If the method of choice is **jortner**, the vibration frequency of the quantum mode has to be given in units of eV. The default value is close to the CC bond-stretch at 0.2eV

Return to the description of `rates`.

4.2.25   sandbox

Sandbox to test xtp classes

option	default	unit	description
ID			Not in use

Return to the description of `sandbox`.

4.2.26 stateserver

Export SQLite file to human readable format

option	default	unit	description
out			*Output file name*
pdb			*PDB coordinate file name*
keys			*Sections to write to readable format (topology, segments, pairs, coordinates)*

Return to the description of `stateserver`.

4.2.27 tdump

Coarse-grained and back-mapped (using rigid fragments) trajectories

option	default	unit	description
md	MD.pdb		*Name of the coarse-grained trajectory*
qm	QM.pdb		*Name of the trajectory with back-substituted rigid fragments*
frames	1		*Number of frames to output*

Return to the description of `tdump`.

4.2.28 vaverage

Computes site-centered velocity averages from site occupancies

option	default	unit	description
carriers			*Carrier types for which to compute velocity averages*
tabulate			*Tabulate 'atoms' or 'segments'*

Return to the description of `vaverage`.

4.2.29 zmultipole

Evaluates polarization contribution based on the Thole model

option	default	unit	description
multipoles			*Polar Site Definitions in GDMA punch-file format*
control			*Control options for induction computation*
induce	1		*Enter '1' / '0' to toggle induction on / off*
first			*First segment for which to compute site energies*
last			*Last segment for which to compute site energies*
output			*File to write site energies to. Site energies are also stored in the state file*
check			*Check mapping of polar sites to fragment*
tholeparam			*Thole parameters required for charge-smearing*
cutoff		nm	*Cut-off beyond which all interactions are neglected*
cutoff2		nm	*Cut-off beyond which polarization is neglected*
expdamp			*Damping exponent used in exponential damping function*
scaling			*1-n interaction scaling, currently not in use*
esp			*Control options for potential calculation*
calcESP			*Enter '1' / '0' to toggle on / off. If '1', site energies will not be evaluated*
cube			
grid			*XYZ file specifying grid points for potential evaluation*
output			*File to write grid-point potential to*

esf			Control options for field calculation
calcESF			Enter '1' / '0' to toggle on / off. If '1', site energies will not be evaluated
grid			XYZ file specifying grid points for field evaluation
output			File to write grid-point field to
alphamol			Control options for molecular-polarizability calculation
calcAlpha			Enter '1' / '0' to toggle on / off. If '1', site energies will not be evaluated
output			File to write polarizability tensor in global frame and in diagonal form to
convparam			Convergence parameters for self-consistent field calculation
wSOR_N			Mixing factor for successive overrelaxation of neutral system, usually between 0.3 and 0.5
wSOR_C			Mixing factor for successive overrelaxation of charged system, usually between 0.3 and 0.5
tolerance			Convergence criterion, fulfilled if relative change smaller than tolerance
maxiter			Maximum number of iterations in the convergence loop

1283 *Return to the description of* `zmultipole`.

4.2.30 edft
1284

calc:edft

1285 *A wrapper for first principles based single site calculations*

option	default	unit	description
job			Job options
tasks	input,run,parse		What to run
store	orbitals		What to store

1286 *Return to the description of* `edft`.

4.2.31 egwbse
1287

calc:egwbse

1288 *An implementation of GW-BSE.*

option	default	unit	description
job			Job options
dftbasis			
gwbasis			
rpamax			
qpmin			
qpmax			
bsemin			
bsemax			
shift			
tasks			
store			
exctotal			
print			

1289 *Return to the description of* `egwbse`.

4.2.32 idft
1290

calc:idft

1291 *Projection method for electronic couplings. Requires edft otput*

option	default	unit	description
tasks	*input,run,parse,t*		*What to do*
store	*orbitals,overlap,in*		*What to store*
degeneracy	*0*	*eV*	*Criterium for the degeneracy of two levels*
levels	*3*		*Output between HOMO, ..., HOMO-levels; LUMO, ..., LUMO+levels*
trim	*2*		*Use trim*occupied of virtual orbitals*

1292 *Return to the description of* `idft`.

4.2.33 igwbse

calc:igwbse
1294 *Projection method for excitonic couplings. Requires gwbse output*

option	default	unit	description
package			
job			
file			
tasks			
gwbse			
dftbasis			
gwbasis			
shift			
tasks			
exctotal			
print			
type	*singlets*		*Spin types for couplings*
degeneracy	*0*	*eV*	*Criterium for the degeneracy of two levels*
states	*5*		*Number of excitons considered*

1295 *Return to the description of* `igwbse`.

4.2.34 qmmm

calc:qmmm
1297 *QM/MM with the Thole MM model*

option	default	unit	description
control			
pdb_check			*PDB file of polar sites*
write_chk	*dipoles.xyz*		*XYZ file with dipoles split onto point charges*
format_chk	*xyz*		*format, gaussian or xyz*
split_dpl	*1*		*'0' do not split dipoles onto point charges, '1' do split*
dpl_spacing	*1e-3*	*nm*	*Spacing to be used when splitting dipole onto point charges: d = q * a*
qmpackage			
package			*QM package to use for the QM region*
gwbse			*Specify if GW/BSE excited state calculation ist needed*
gwbse_options			*GW/BSE options file*
state			*Number of excited state, which is to be calculated*
type			*Character of the excited state to be calculated*
filter			*Filter with which to find the excited state after each calculation*
oscillator_strength			*Oscillator strength filter, only states with higher oscillator strength are considered*
charge_transfer			*Charge transfer filter , only states with charge transfer above threshold are consdered*
qmmmconvg			*convergence criteria for the QM/MM*
dR	*0.001*	*nm*	*RMS of coordinates*

dQ	*0.001*	*e*	*RMS of charges*
dE_QM	*0.0001*	*eV*	*Energy change of the QM region*
dE_MM	*0.0001*	*eV*	*Energy change of the MM region*
max_iter	*10*		*Number of iterations*
coulombmethod			*Options for the MM embedding*
method	*cut-off*		*Method for evaluation of electrostatics*
cutoff1			*Cut-off for the polarizable MM1 shell*
cutoff2			*Cut-off for the static MM2 shell*
tholemodel			*Parameters for teh Thole model*
induce			*'1' - induce '0' - no induction*
induce_intra_pair			*'1' - include mutual interaction of induced dipoles in the QM region. '0' - do not*
exp_damp	*0.39*		*Sharpness parameter*
scaling			*Bond scaling factors*
convergence			*Convergence parameters for the MM1 (polarizable) region*
wSOR_N			*Mixing factor for the succesive overrelaxation algorithm for a neutral QM region*
wSOR_C			*Mixing factor for the succesive overrelaxation algorithm for a charged QM region*
max_iter	*512*		*Maximal number of iterations to converge induced dipoles*
tolerance			*Maximum RMS change allowed in induced dipoles*

1298   *Return to the description of* qmmm.

4.2.35   xqmultipole

1299

calc:xqmultipole
1300   *Electrostatic interaction and induction energy of charged molecular clusters*

option	default	unit	description
multipoles			*Polar-site mapping definition*
control			
job_file			*Job file*
emp_file			*Polar-background definition, allocation of mps-files to segments*
pdb_check			*Whether or not to output a pdb-file of the mapped polar sites*
format_chk			*Format for check-file: 'xyz' or 'gaussian'*
split_dpl			*Split dipoles onto point charges in check-file*
dpl_spacing		*nm*	*Spacing between point charges for check-file output*
coulombmethod			
method			*Currently only cut-off supported*
cutoff1		*nm*	*Full-interaction radius cut-off*
cutoff2		*nm*	*Radius of electrostatic buffer*
tholemodel			
induce			*Induce - or not*
induce_intra_pair			*Induce mutually within the charged cluster*
exp_damp			*Thole sharpness parameter*
scaling			*Bond scaling parameters, currently not used*
convergence			
wSOR_N			*SOR mixing factor for overall neutral clusters*
wSOR_C			*SOR mixing factor for overall charged clusters*
max_iter			*Maximum number of iterations*
tolerance			*Relative tolerance as convergence criterion*

1301   *Return to the description of* xqmultipole.

4.2.36   energy2xml

1302

calc:energy2xml
1303   *Write out energies from SQL file*

option	default	unit	description

1304 *Return to the description of* `energy2xml`*.*

4.2.37 integrals2xml

calc:integrals2xml

1306 *Write out transfer integrals from SQL file*

option	default	unit	description

1307 *Return to the description of* `integrals2xml`*.*

4.2.38 occupations2xml

calc:occupations2xml

1309 *Write out site occupation probabilities from SQL file*

option	default	unit	description

1310 *Return to the description of* `occupations2xml`*.*

4.2.39 pairs2xml

calc:pairs2xml

1312 *Write out neighbourlist from SQL file*

option	default	unit	description

1313 *Return to the description of* `pairs2xml`*.*

4.2.40 rates2xml

calc:rates2xml

1315 *Write out charge transfer rates from SQL file*

option	default	unit	description

1316 *Return to the description of* `rates2xml`*.*

4.2.41 segments2xml

calc:segments2xml

1318 *Write out segment data from SQL file*

option	default	unit	description

1319 *Return to the description of* `segments2xml`*.*

4.2.42 trajectory2pdb

calc:trajectory2pdb

1321 *Generate PDB files for the mapped MD/QM topology*

option	default	unit	description

1322 *Return to the description of* `trajectory2pdb`*.*

1323 4.3   Common options

ref:options

name	Description of the option

Bibliography

ruhle_microscopic_2011 [1] V. Rühle et al., *J. Chem. Theory Comput.* **7**, 3335 (2011). *ii*, *3*, *17*, *18*

ruhle_versatile_2009 [2] V. Rühle et al., *J. Chem. Theory Comput.* **5**, 3211 (2009). *ii*, *3*, *6*

gamma_design_1995 [3] E. Gamma, R. Helm, and R. E. Johnson, Design Patterns. Elements of Reusable Object-Oriented Software., *1st ed., reprint. ed. (Addison-Wesley Longman, Amsterdam, ADDRESS, 1995). 3*

ruhle_multiscale_2010 [4] V. Rühle, J. Kirkpatrick, and D. Andrienko, *J. Chem. Phys.* **132**, 134103 (2010). *7*

vukmirovic_charge_2008 [5] N. Vukmirović and L.-W. Wang, *J. Chem. Phys.* **128**, 121102 (2008). *7*

vukmirovic_charge_2009 [6] N. Vukmirović and L.-W. Wang, *Nano Letters* **9**, 3996 (2009).

mcmahon_ad_2009 [7] D. P. McMahon and A. Troisi, *Chem. Phys. Lett.* **480**, 210 (2009). *7*

bredas_charge-transfer_2004 [8] J.-L. Brédas, D. Beljonne, V. Coropceanu, and J. Cornil, *Chem. Rev.* **104**, 4971 (2004). *8*, *17*

breneman_determining_1990 [9] C. M. Breneman and K. B. Wiberg, *J. Comput. Chem.* **11**, 361–373 (1990). *10*

stone_distributed_1985 [10] A. Stone and M. Alderton, *Molecular Physics* **56**, 1047 (1985). *10*, *11*

chirlian_atomic_1987 [11] L. E. Chirlian and M. M. Francl, *J. Comput. Chem.* **8**, 894 (1987). *10*

singh_approach_1984 [12] U. C. Singh and P. A. Kollman, *J. Comput. Chem.* **5**, 129 (1984). *11*

stone_distributed_2005 [13] A. J. Stone, *J. Chem. Theory Comput.* **1**, 1128 (2005). *11*

stone_theory_1997 [14] A. J. Stone, The Theory of intermolecular forces *(Clarendon Press, Oxford, 1997). 11*

thole_molecular_1981 [15] B. Thole, *Chem. Phys.* **59**, 341 (1981). *12*

ren_polarizable_2003 [16] P. Ren and J. W. Ponder, *J. Phys. Chem. B* **107**, 5933 (2003). *12*, *13*

troisi_charge-transport_2006 [17] A. Troisi and G. Orlandi, *Phys. Rev. Lett.* **96**, (2006). *13*

troisi_charge_2009 [18] A. Troisi, D. L. Cheung, and D. Andrienko, *Phys. Rev. Lett.* **102**, 116602 (2009).

mcmahon_organic_2010 [19] D. P. McMahon and A. Troisi, *ChemPhysChem* **11**, 2067 (2010). *13*

baumeier_density-functional_2010 [20] B. Baumeier, J. Kirkpatrick, and D. Andrienko, *Phys. Chem. Chem. Phys.* **12**, 11103 (2010). *13*, *16*, *17*

kirkpatrick_approximate_2008 [21] J. Kirkpatrick, *Int. J. Quantum Chem.* **108**, 51 (2008). *17*

walker_electrical_2002 [22] A. B. Walker, A. Kambili, and S. J. Martin, *J. Phys-Condens. Mat.* **14**, 9825 (2002). *17*

baessler_charge_1993 [23] H. Baessler, *Phys. Status Solidi B* **175**, 15 (1993).

borsenberger_charge_1991 [24] P. M. Borsenberger, L. Pautmeier, and H. Bässler, *J. Chem. Phys.* **94**, 5447 (1991).

pasveer_unified_2005 [25] W. F. Pasveer et al., *Phys. Rev. Lett.* **94**, 206601 (2005). *17*

bredas_molecular_2009 [26] J.-L. Brédas, J. E. Norton, J. Cornil, and V. Coropceanu, *Accounts Chem. Res.* **42**, 1691 (2009). *17*

coropceanu_charge_2007 [27] V. Coropceanu et al., *Chem. Rev.* **107**, 926 (2007).

nelson_modeling_2009 [28] J. Nelson, J. J. Kwiatkowski, J. Kirkpatrick, and J. M. Frost, *Accounts Chem. Res.* **42**, 1768 (2009). *17*

marcus_electron_1993 [29] R. A. Marcus, *Rev. Mod. Phys.* **65**, 599 (1993). *17*

hutchison_hopping_2005   *[30] G. R. Hutchison, M. A. Ratner, and T. J. Marks, J. Am. Chem. Soc.* **127***, 2339 (2005).* *17*

chang_new_2005   *[31] J.-L. Chang, J. Mol. Spectrosc.* **232***, 102 (2005).* *18*

hoffman_reorganization_1996   *[32] B. M. Hoffman and M. A. Ratner, Inorg. Chim. Acta.* **243***, 233 (1996).* *18*

bortz_new_1975   *[33] A. B. Bortz, M. H. Kalos, and J. L. Lebowitz, J. Comput. Phys.* **17***, 10 (1975).* *19*

scher_anomalous_1975   *[34] H. Scher and E. Montroll, Phys. Rev. B* **12***, 2455 (1975).* *19*

borsenberger_role_1993   *[35] P. M. Borsenberger, E. H. Magin, M. D. VanAuweraer, and F. C. D. Schryver, Phys. Status Solidi A* **140***, 9 (1993).* *19*

derrida_velocity_1983   *[36] B. Derrida, J. Stat. Phys.* **31***, 433 (1983).* *19*, *21*

cordes_one-dimensional_2001   *[37] H. Cordes et al., Phys. Rev. B* **63***, 094201 (2001).*

seki_electric_2001   *[38] K. Seki and M. Tachiya, Phys. Rev. B* **65***, 014305 (2001).* *19*

lukyanov_extracting_2010   *[39] A. Lukyanov and D. Andrienko, Phys. Rev. B* **82***, 193202 (2010).* *19*

van_der_holst_modeling_2009   *[40] J. J. M. van der Holst et al., Phys. Rev. B* **79***, 085203 (2009).* *21*

dunlap_charge-dipole_1996   *[41] D. Dunlap, P. Parris, and V. Kenkre, Phys. Rev. Lett.* **77***, 542 (1996).* *21*

novikov_essential_1998   *[42] S. V. Novikov et al., Phys. Rev. Lett.* **81***, 4472 (1998).* *21*

nagata_atomistic_2008   *[43] Y. Nagata and C. Lennartz, J. Chem. Phys.* **129***, 034709 (2008).* *21*

novikov_cluster_1995   *[44] S. V. Novikov and A. V. Vannikov, J. Phys. Chem.* **99***, 14573 (1995).* *21*